FINAL TECHNICAL REPORT

FIBER OPTIC LASER

Elias Snitzer

May 1965

USAROD Project No. 3209
Contract No. DA-19-020-AMC-0160(X)

U. S. Army Research Office
Durham, North Carolina

Research Division
American Optical Company
Southbridge, Massachusetts

AD ______________ Accession No. ______________

American Optical Company, Research Division, Southbridge, Massachusetts.

FIBER OPTIC LASER — E. Snitzer

Final Technical Report, May 1965, 72 pp, 29 illus, Contract DA-19-020-AMC-0160(X) — Unclassified Report

The problems of frequency control of a neodymium glass laser and the broadening mechanisms involved in neodymium fluorescence and laser action in glass are considered. It is found that laser emission can be obtained in narrow lines less than 0.1A wide anywhere within 130A wide interval centered about the peak emission at 1.0585A by the use of thin reflecting plates acting as wavelength sensitive mode selectors. Spontaneous emission of Nd^{3+} in glass at 1.06 μ has a full width at half maximum of 180A, which is nearly independent of temperature. From time resolved spectral studies of clad rods as functions of pump power, temperature, Nd^{3+} concentration, and cavity Q, it is concluded that the 180A wide line consists of overlapping ligand field split lines, the central portion of which has a half width of approximately 65A. From the hole burning observed in the time resolved spectra the homogeneous line width at room temperature is about 20A and reduces to 5A at 77°K.

UNCLASSIFIED

1. Lasers; Fiber Optics
2. Contract DA-19-020-AMC-0160(X)
3. U. S. Army Research Office, Durham

UNCLASSIFIED

AD ______________ Accession No. ______________

American Optical Company, Research Division, Southbridge, Massachusetts.

FIBER OPTIC LASER — E. Snitzer

Final Technical Report, May 1965, 72 pp, 29 illus, Contract DA-19-020-AMC-0160(X) — Unclassified Report

The problems of frequency control of a neodymium glass laser and the broadening mechanisms involved in neodymium fluorescence and laser action in glass are considered. It is found that laser emission can be obtained in narrow lines less than 0.1A wide anywhere within 130A wide interval centered about the peak emission at 1.0585A by the use of thin reflecting plates acting as wavelength sensitive mode selectors. Spontaneous emission of Nd^{3+} in glass at 1.06 μ has a full width at half maximum of 180A, which is nearly independent of temperature. From time resolved spectral studies of clad rods as functions of pump power, temperature, Nd^{3+} concentration, and cavity Q, it is concluded that the 180A wide line consists of overlapping ligand field split lines, the central portion of which has a half width of approximately 65A. From the hole burning observed in the time resolved spectra the homogeneous line width at room temperature is about 20A and reduces to 5A at 77°K.

UNCLASSIFIED

1. Lasers; Fiber Optics
2. Contract DA-19-020-AMC-0160(X)
3. U. S. Army Research Office, Durham

UNCLASSIFIED

AD ______________ Accession No. ______________

American Optical Company, Research Division, Southbridge, Massachusetts.

FIBER OPTIC LASER — E. Snitzer

Final Technical Report, May 1965, 72 pp, 29 illus, Contract DA-19-020-AMC-0160(X) — Unclassified Report

The problems of frequency control of a neodymium glass laser and the broadening mechanisms involved in neodymium fluorescence and laser action in glass are considered. It is found that laser emission can be obtained in narrow lines less than 0.1A wide anywhere within 130A wide interval centered about the peak emission at 1.0585A by the use of thin reflecting plates acting as wavelength sensitive mode selectors. Spontaneous emission of Nd^{3+} in glass at 1.06 μ has a full width at half maximum of 180A, which is nearly independent of temperature. From time resolved spectral studies of clad rods as functions of pump power, temperature, Nd^{3+} concentration, and cavity Q, it is concluded that the 180A wide line consists of overlapping ligand field split lines, the central portion of which has a half width of approximately 65A. From the hole burning observed in the time resolved spectra the homogeneous line width at room temperature is about 20A and reduces to 5A at 77°K.

UNCLASSIFIED

1. Lasers; Fiber Optics
2. Contract DA-19-020-AMC-0160(X)
3. U. S. Army Research Office, Durham

UNCLASSIFIED

AD ______________ Accession No. ______________

American Optical Company, Research Division, Southbridge, Massachusetts.

FIBER OPTIC LASER — E. Snitzer

Final Technical Report, May 1965, 72 pp, 29 illus, Contract DA-19-020-AMC-0160(X) — Unclassified Report

The problems of frequency control of a neodymium glass laser and the broadening mechanisms involved in neodymium fluorescence and laser action in glass are considered. It is found that laser emission can be obtained in narrow lines less than 0.1A wide anywhere within 130A wide interval centered about the peak emission at 1.0585A by the use of thin reflecting plates acting as wavelength sensitive mode selectors. Spontaneous emission of Nd^{3+} in glass at 1.06 μ has a full width at half maximum of 180A, which is nearly independent of temperature. From time resolved spectral studies of clad rods as functions of pump power, temperature, Nd^{3+} concentration, and cavity Q, it is concluded that the 180A wide line consists of overlapping ligand field split lines, the central portion of which has a half width of approximately 65A. From the hole burning observed in the time resolved spectra the homogeneous line width at room temperature is about 20A and reduces to 5A at 77°K.

UNCLASSIFIED

1. Lasers; Fiber Optics
2. Contract DA-19-020-AMC-0160(X)
3. U. S. Army Research Office, Durham

UNCLASSIFIED

AD _____ Accession No. _____

American Optical Company, Research Division, Southbridge, Massachusetts.

FIBER OPTIC LASER E. Snitzer

Final Technical Report, May 1965, 72 pp, 29 illus, Contract DA-19-020-AMC-0160(X) Unclassified Report

The problems of frequency control of a neodymium glass laser and the broadening mechanisms involved in neodymium fluorescence and laser action in glass are considered. It is found that laser emission can be obtained in narrow lines less than 0.1A wide anywhere within 130A wide interval centered about the peak emission at 1.0585A by the use of thin reflecting plates acting as wavelength sensitive mode selectors. Spontaneous emission of Nd^{3+} in glass at 1.06 μ has a full width at half maximum of 180A, which is nearly independent of temperature. From time resolved spectral studies of clad rods as functions of pump power, temperature, Nd^{3+} concentration, and cavity Q, it is concluded that the 180A wide line consists of overlapping ligand field split lines, the central portion of which has a half width of approximately 65A. From the hole burning observed in the time resolved spectra the homogeneous line width at room temperature is about 20A and reduces to 5A at 77°K.

UNCLASSIFIED

1. Lasers; Fiber Optics
2. Contract DA-19-020-AMC-0160(X)
3. U. S. Army Research Office, Durham

UNCLASSIFIED

AD _____ Accession No. _____

American Optical Company, Research Division, Southbridge, Massachusetts.

FIBER OPTIC LASER E. Snitzer

Final Technical Report, May 1965, 72 pp, 29 illus, Contract DA-19-020-AMC-0160(X) Unclassified Report

The problems of frequency control of a neodymium glass laser and the broadening mechanisms involved in neodymium fluorescence and laser action in glass are considered. It is found that laser emission can be obtained in narrow lines less than 0.1A wide anywhere within 130A wide interval centered about the peak emission at 1.0585A by the use of thin reflecting plates acting as wavelength sensitive mode selectors. Spontaneous emission of Nd^{3+} in glass at 1.06 μ has a full width at half maximum of 180A, which is nearly independent of temperature. From time resolved spectral studies of clad rods as functions of pump power, temperature, Nd^{3+} concentration, and cavity Q, it is concluded that the 180A wide line consists of overlapping ligand field split lines, the central portion of which has a half width of approximately 65A. From the hole burning observed in the time resolved spectra the homogeneous line width at room temperature is about 20A and reduces to 5A at 77°K.

UNCLASSIFIED

1. Lasers; Fiber Optics
2. Contract DA-19-020-AMC-0160(X)
3. U. S. Army Research Office, Durham

UNCLASSIFIED

AD _____ Accession No. _____

American Optical Company, Research Division, Southbridge, Massachusetts.

FIBER OPTIC LASER E. Snitzer

Final Technical Report, May 1965, 72 pp, 29 illus, Contract DA-19-020-AMC-0160(X) Unclassified Report

The problems of frequency control of a neodymium glass laser and the broadening mechanisms involved in neodymium fluorescence and laser action in glass are considered. It is found that laser emission can be obtained in narrow lines less than 0.1A wide anywhere within 130A wide interval centered about the peak emission at 1.0585A by the use of thin reflecting plates acting as wavelength sensitive mode selectors. Spontaneous emission of Nd^{3+} in glass at 1.06 μ has a full width at half maximum of 180A, which is nearly independent of temperature. From time resolved spectral studies of clad rods as functions of pump power, temperature, Nd^{3+} concentration, and cavity Q, it is concluded that the 180A wide line consists of overlapping ligand field split lines, the central portion of which has a half width of approximately 65A. From the hole burning observed in the time resolved spectra the homogeneous line width at room temperature is about 20A and reduces to 5A at 77°K.

UNCLASSIFIED

1. Lasers; Fiber Optics
2. Contract DA-19-020-AMC-0160(X)
3. U. S. Army Research Office, Durham

UNCLASSIFIED

AD _____ Accession No. _____

American Optical Company, Research Division, Southbridge, Massachusetts.

FIBER OPTIC LASER E. Snitzer

Final Technical Report, May 1965, 72 pp, 29 illus, Contract DA-19-020-AMC-0160(X) Unclassified Report

The problems of frequency control of a neodymium glass laser and the broadening mechanisms involved in neodymium fluorescence and laser action in glass are considered. It is found that laser emission can be obtained in narrow lines less than 0.1A wide anywhere within 130A wide interval centered about the peak emission at 1.0585A by the use of thin reflecting plates acting as wavelength sensitive mode selectors. Spontaneous emission of Nd^{3+} in glass at 1.06 μ has a full width at half maximum of 180A, which is nearly independent of temperature. From time resolved spectral studies of clad rods as functions of pump power, temperature, Nd^{3+} concentration, and cavity Q, it is concluded that the 180A wide line consists of overlapping ligand field split lines, the central portion of which has a half width of approximately 65A. From the hole burning observed in the time resolved spectra the homogeneous line width at room temperature is about 20A and reduces to 5A at 77°K.

UNCLASSIFIED

1. Lasers; Fiber Optics
2. Contract DA-19-020-AMC-0160(X)
3. U. S. Army Research Office, Durham

UNCLASSIFIED

FOREWORD

This report was prepared by the Research Division, American Optical Company, Southbridge, Massachusetts, on Army contract DA-19-020-AMC-0160(X) Fiber Optic Laser under project number 3209 of the Army Research Office (Durham). Project monitor for Durham was Dr. Herman Robl.

Project Director for the Research Division was Dr. E. Snitzer. Contributors to the program included Mr. R. W. Young, Dr. W. Prindle, and Mr. L. O. Upton, preparation of the glass samples; Mr. C. Yates, grinding and polishing of the samples; Dr. H. Jupnik and Mr. C. Colwell, evaporations; Mr. W. Bazinet, Mr. D. Cuff and Mr. H. Cole, preparation of fibers and fiber bundles; and Mr. R. Lavallee, assistance with electronics and instrumentation. Laboratory work was done by Mr. F. Hoffman, Mr. N. Guertin and Mr. R. Crevier.

This report is the final report and it concludes the work on Contract DA-19-020-AMC-0160(X). It also includes research performed under Contract DA-19-020-ORD-5575.

The report is unclassified.

ABSTRACT

The problems of frequency control of a neodymium glass laser and the broadening mechanisms involved in neodymium fluorescence and laser action in glass are considered. It is found that laser emission can be obtained in narrow lines less than 0.1A wide anywhere within 130A wide interval centered about the peak emission at 1.0585A by the use of thin reflecting plates acting as wavelength sensitive mode selectors. Spontaneous emission of Nd^{3+} in glass at 1.06μ has a full width at half maximum of 180A, which is nearly independent of temperature. From time resolved spectral studies of clad rods as functions of pump power, temperature, Nd^{3+} concentration, and cavity Q, it is concluded that the 180A wide line consists of overlapping ligand field split lines, the central portion of which has a half width of approximately 65A. From the hole burning observed in the time resolved spectra the homogeneous line width at room temperature is about 20A and reduces to 5A at 77°K.

TABLE OF CONTENTS

ILLUSTRATIONS

ILLUSTRATIONS (cont.)

I. INTRODUCTION

Since the development of laser glasses, and in particular the neodymium glass, the most feasible fiber lasers were those made from glass. Many of the problems associated with fiber lasers are common to larger, more conventional, geometries. The properties of fiber configurations are being extensively studied in other programs at the American Optical Company such as Contract #AF30(602)-3389. Hence, the major concern of the present contract has been with the materials aspects of neodymium glass lasers.

A feature which is peculiar to the glassy hosts is the inhomogeneous broadening of the fluorescent lines. The normal fluorescent emission centered at approximately 1.06μ has a temperature independent line width of 180A at half maximum. The problems of hole burning and the homogeneous line width were investigated by time resolved spectral studies of clad rods. By the use of thin reflecting plates which behave as frequency sensitive mode selectors, it is possible to obtain laser action in narrow lines anywhere within 130A.

II. FREQUENCY CONTROL WITH REFLECTING PLATES

A. Background

The spectrum of a 1.06μ neodymium glass laser can be in the form of sharp lines or broad bands.[1] The wavelength interval over which laser action occurs is a function of pump power. Just above threshold the laser emission is over only a few Angstroms and with increasing pump power can be as wide as 130 Angstroms. By the inclusion of a thin plate within the resonant cavity to act as a transmission filter the laser emission in ruby was shown to narrow.[2] Line narrowing of the laser emission in glass has also been produced by the use of a thin plate as a reflection filter.[1] One of the end reflectors of the laser rod is replaced by the thin plate. Here, the results are presented of experiments on line narrowing of a neodymium glass laser with a reflection filter, transmission filter, or both.

B. Reflectivity of a plate

The reflectivity R at normal incidence at the wavelength λ of a plate of thickness D and index of refraction n is given by[3]

$$R = \frac{(r_1^{\frac{1}{2}} - r_2^{\frac{1}{2}})^2 + 4\,(r_1 r_2)^{\frac{1}{2}} \sin^2\phi}{(1 - (r_1 r_2)^{\frac{1}{2}})_2 + 4\,(r_1 r_2)^{\frac{1}{2}} \sin^2\phi} \qquad (1)$$

where

$$\phi = 2\pi nD/\lambda \qquad (2)$$

and r_1 and r_2 are the reflectivities of the two surfaces. Possible

phase displacements at the surfaces due to the coatings to produce the reflectivities r_1 and r_2 have been neglected. If the light is incident at the angle θ with respect to the normal to the plate, D in Eq. (2) is replaced by D cos θ.

With the reflectivities of the two surfaces taken equal to r the above becomes

$$R = 4r \sin^2 \phi / \left[(1-r)^2 + 4r \sin^2 \phi \right] \qquad (3)$$

In Fig. 1 are plotted the reflectivity R as a function of the phase ϕ for several values of the surface reflectivity r. For wavelengths at which the thickness of the plate is equal to an even number of quarter wavelengths the reflectivity is zero. When the plate is an odd number of quarter wavelengths the reflectivity of the plate is a maximum.

From Eq. (2) the wavelength interval $\Delta\lambda$ between maxima in R or between the values of λ at which R = 0 is given by

$$\Delta\lambda = \lambda^2 / 2nD \qquad (4)$$

If a tilted or canted plate is placed between the laser rod and a removed end reflector it is the transmission characteristics of the thin plate which serves to give a high Q at those wavelengths for which the plate is an even number of quarter wavelengths.

By using the plate as a removed end reflector, laser emission is preferred at the wavelengths at which the plate thickness is an odd

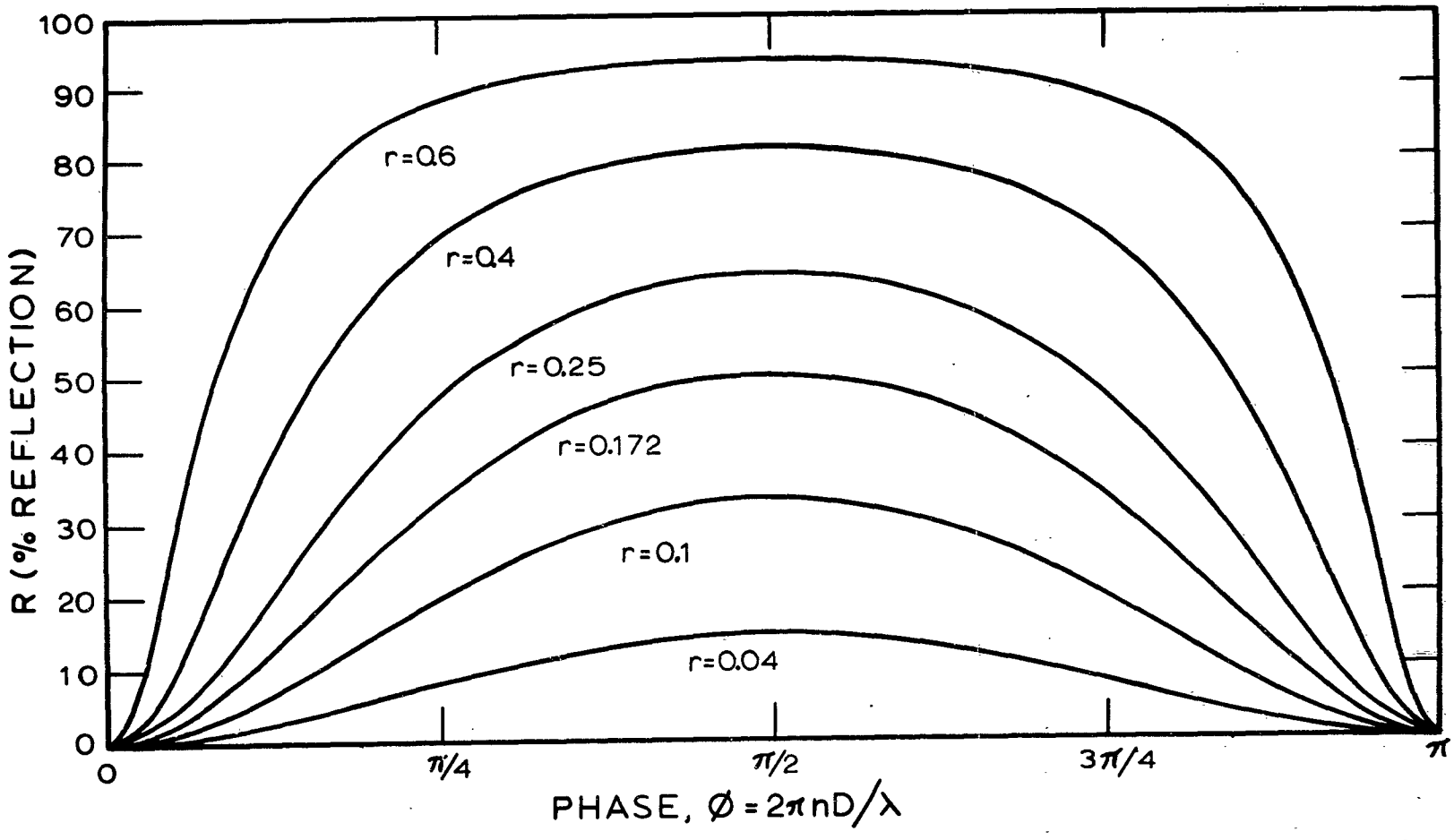

FIGURE 1. The total reflectivity R at the wavelength λ of a plate of thickness D for various values of the surface reflectivity r.

number of $\lambda/4$.

If both an aligned plate and a tilted plate are used one obtains a frequency selective characteristic which is given by the product of the reflectivity of the aligned plate and the transmissivity of the tilted plate.

The reflectivity of the surfaces of the plate influences its mode selective properties. In a tilted plate the higher the reflectivity of the two surfaces the narrower the band pass characteristic. In the case of the aligned plate, too high a reflectivity gives a broad maximum for the total reflectivity and hence in the Q as a function of λ. If the reflectivity is too low for the aligned plate there is also obviously a very broad reflection characteristic. To find the optimum reflectivity for the aligned plate and to provide a convenient measure of the frequency selective characteristic so as to compare the aligned and tilted plates the second derivatives at the peaks can be obtained. The results are

$$R''(\phi=0) = (2\pi nD/c)^2 8r/(1-r)^2 \tag{5}$$

$$R''(\phi=\pi/2) = -(2\pi nD/c)^2 8r(1-r)^2/(1-r)^4 \tag{6}$$

The primes on R refer to differentiation with respect to the frequency ν.

From Eq. (4), R'' at $\phi = 0$ increases for increasing values of r through the whole range of possible reflectivities r. The value of

$|R''|$ at $\phi = \pi/4$ goes through a maximum at $r = 0.172$, at which the total reflectivity is $R = 0.5$.

Thus far the reflectivity of the exit end of the laser rod has not been taken into account. If the plate is parallel to the end of the rod the total reflectivity is due to coherent reflections from all three surfaces. However, the rod surface can simply add incoherently to the reflectivity of the plate if the surfaces are not aligned or if the beam spread is large so that the angle of a ray with respect to the axis is not well defined.

Let the reflectivity of the end of the rod be s and the spacing between rod and plate be D'. The plate has a thickness D and for simplicity its two surfaces are assumed to have the same reflectivity r. The total reflectivity for a plane wave that makes the angle θ' with respect to the axis is given by[4]

$$R = (A + sB - s^{\frac{1}{2}}C)/(sA + B - s^{\frac{1}{2}}C), \tag{7}$$

where

$$A = 4r \sin^2\varphi,$$

$$B = (1-r)^2 + 4r \sin^2\varphi,$$

$$C = 4r^{\frac{1}{2}} \sin\varphi \left[\sin(2\varphi' + \varphi) - r \sin(2\varphi' - \varphi)\right],$$

$$\varphi' = 2\pi D' \cos\theta'/\lambda \tag{8}$$

In using Eq. (7) three typical behaviors can be distinguished. The simplest situation is where $s \ll r$ and Eq. (7) reduces to Eq. (3). This would be the case if the end of the rod had an anti-reflection coating on it or if it were cut at Brewster's angle. In the other

two cases s = r but the reflectivities from the plate and rod add coherently or incoherently. An incoherent addition can be viewed as resulting from an average of Eq. (7) over φ'. For small values of r and s the incoherent addition is equivalent to replacing Eq. (7) by the sum of s and the value of R given by Eq. (3).

If $D' >> D$, the total reflectivity shown in Fig. 1 would have a superimposed oscillation whose period is given by Eq. (8). For example, if the plate and rod surfaces have only the Fresnel reflection for a material with an index of refraction of 1.5, the values of r and s are 0.04. For $\varphi = 0$, R = 0.04 irrespective of the value of φ'. For $\varphi = \pi/2$, R fluctuates between 0.053 at $\varphi' = 0$ and 0.287 at $\varphi' = \pi/2$. If an anti-reflection coating is used on the rod, Eq. (3) gives R = 0 at $\varphi = 0$ and R = 0.148 at $\varphi = \pi/4$. In Fig. 2 is shown the reflectivity obtained from Eq.(7) with $D' = 20D$ and r = s = 0.04; the value of R from Eq. (3) is shown dotted.

The frequency selectivity provided by a tilted plate with highly reflecting surfaces is considerably better than that obtainable with an aligned plate. However, if the optical quality of the laser is not exceptionally good and, furthermore, does not change during the process of lasing, the mode selection provided by the tilted plate could be so high that most of the energy is lost by being reflected out of the beam. This is typical of mode selection problems. The more selective the geometry the tighter the tolerance in order not to drastically reduce the laser output. On the other hand the aligned plate that

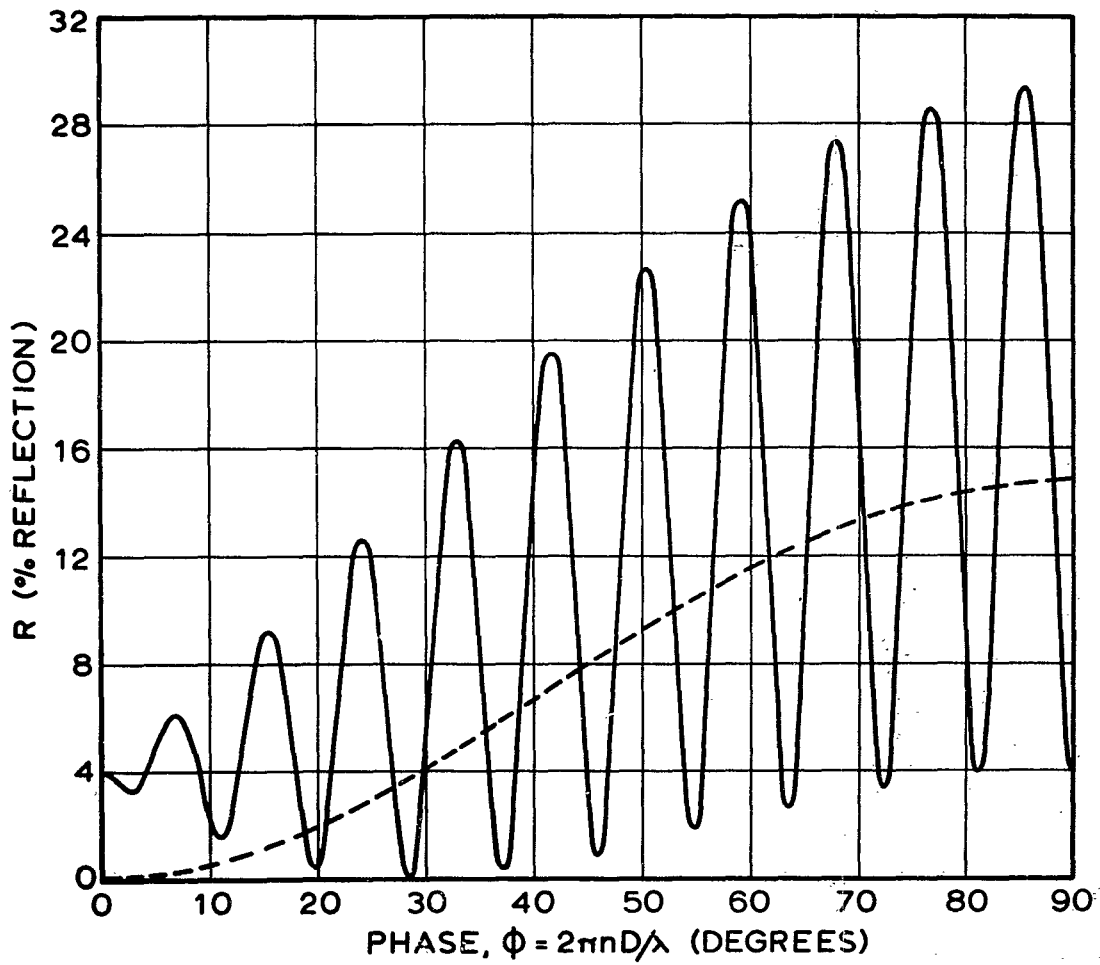

FIGURE 2. The reflectivity of a plate of thickness D as a function of wavelength λ for the plate a distance 20D from the end of the rod. The rod surface and the two plate surfaces have the reflectivity s=r=0.04. For comparison the dotted line shows the reflectivity for the plate only.

depends on transmission will not cause the laser to lose any output light. Instead, if the optical quality is not good enough the laser line tends to broaden. This is because failure to meet the mode selection characteristics precisely cannot remove light from the beam but instead permits other wavelengths to lase. To summarize, limitations imposed by optical imperfections in the cavity for the tilted plate results in reduced intensity but no reduction in monochromaticity. Whereas, the reverse is the case for the aligned plate. If both the aligned and tilted plates are used some immediate condition results..

C. Experimental Results

The laser rods used were 1/4 inch diameter and 18 inches long. One end had a full reflector, either evaporated silver or a roof prism. The exit end had only the 4% Fresnel reflection for a glass air interface. Some of the rods were clad with a clear glass of lower refractive index and with a polished interface between the Nd^{3+} glass core and the cladding. The unclad rods gave narrow beam spreads, random spiking in the time trace and many sharp lines in the spectrum.

For the clad rods a large number of modes are available for excitation. If the glass is relatively striated these modes are all coupled. Discrete standing waves are not recognized. The laser output consists of wide beams (typically 10° to 15° for the index of refraction combinations used for the core and cladding), a damped oscillation in the time trace and broad bands in the spectrum. The broad bands were several Angstroms wide and 5 to 20 Angstroms apart. In some clad rods

part of the output is in the form of broad bands and part in sharp spectral lines.

In Fig. 3 are the spectra for various pump powers for a glass plate with a thickness of 0.63 mm. The plate was not particularly good. The surfaces were flat to about one fringe in the green but the parallelism was poor (10 fringes/cm). In Fig. 3(a) the plate was placed 4 cm from the exit end of a clad rod with a broad beam spread. In Fig. 3(b) the spectra were taken with the plate 4 cm in front of a rod with a narrow beam spread. Neither the plate surfaces nor the exit end of the laser rods were coated. The pictures were taken by imaging the reflecting plate onto the entrance slit of a Jarrell-Ash Model 70-000, 3.4 meter spectrograph.

From Fig. 3 it is clear that wavelength selectively is more effectively accomplished in a clad rod with a wide beam than with a narrow beam, unclad rod. In the latter case, laser emission occurs at those frequencies for which a standing wave is established in both the plate and the laser rod. Within the broad maximum of the total reflectivity of the plate there can be several frequencies at which standing waves in the rod make laser action possible. Furthermore, the non-uniform thickness of the plate would tend to excite many modes; this is probably responsible for the patchy character of the lines. On the other hand, the clad rod gives quite narrow and reproducible laser emission lines. The width of the lines shown in Fig. 3(a) were all less than 0.1 A. Laser action begins at the peaks of the R curve. Since there

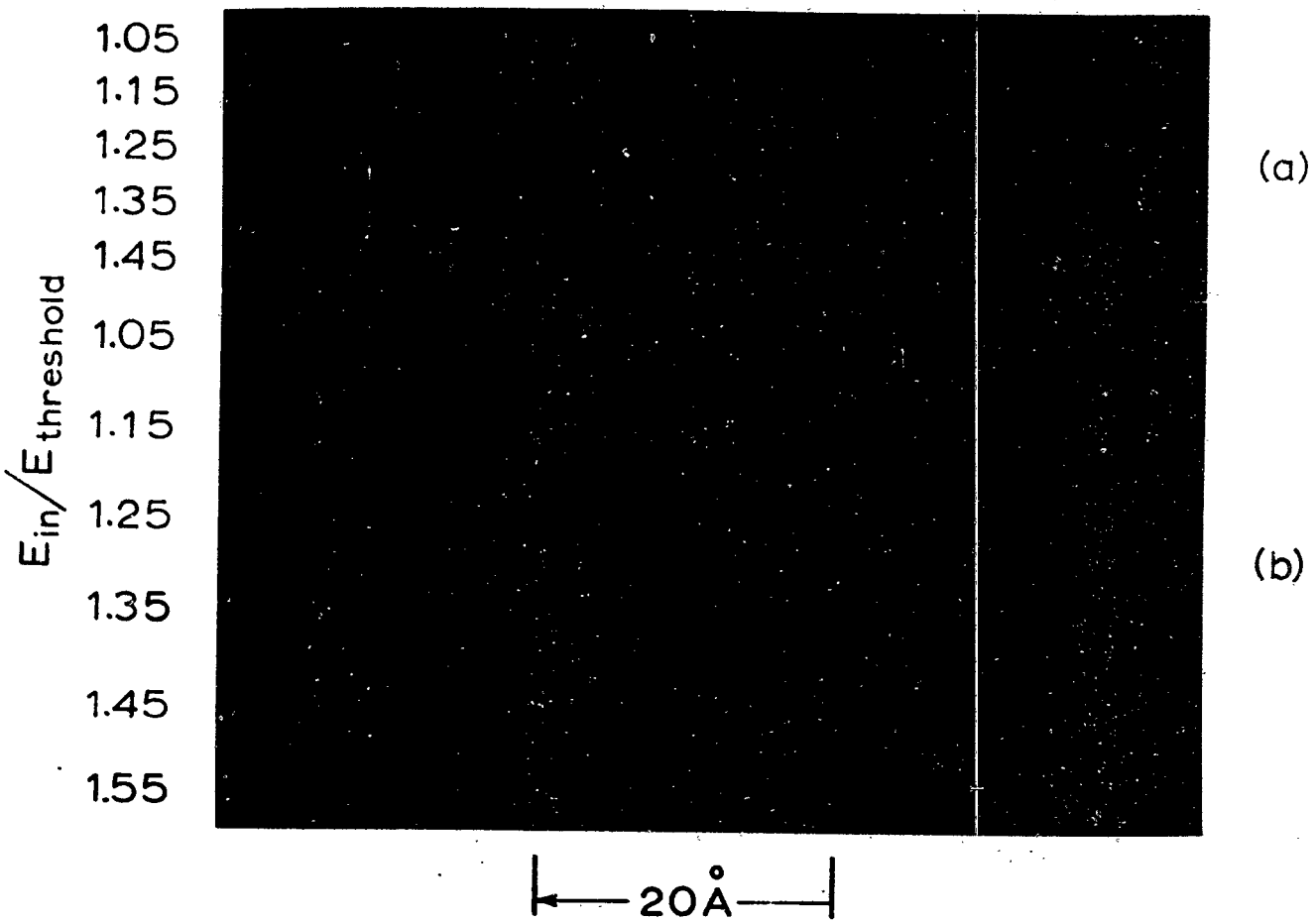

FIGURE 3. Spectra at various pump powers for a 0.63mm thick glass plate 4cm from the end of the laser rod. A clad laser rod was used in (a) and an unclad narrow beam laser used in (b).

are no critical standing waves established in the rod, there is no tendency for the wavelength of emission to hop from mode to mode. Furthermore, the non-uniformity of the plate is not a particular problem for the wide beam spread tends to average over the plate surface. At whatever wavelength a maximum of light is returned from the plate back into the rod within its acceptance angle is the wavelength at which laser emission occurs.

In Fig. 4 are shown the spectra for thin glass and mica plates with a narrow beam, unclad laser rod. The glass thicknesses were uniform to less than $\lambda/4$ and the mica substantially better than this. In such thin sections there was too much flexure to speak meaningfully of the flatness. For the glass plates laser emission occurs in several lines with the interval increasing for the thinner plates.

For the mica plate the increase in linewidth with increasing pump power is due to heating up of the mica during laser emission. This was established by obtaining the spectra at various temperatures of the mica with the laser operated just above threshold. There is also agreement with the calculated temperature rise due to absorption by the mica. A shift of 0.13A/°C was found. For the mica pumped 2.5 times threshold, there is a shift toward longer wavelengths of 7.5A. This corresponds to a temperature rise of 58°C. The absorption coefficient at 1.06 microns of a 0.017" thick piece of similar mica was measured as 23%/mm. Neglecting the effect of multiple reflections the 0.15 mm sample would absorb 3.5% of the incident beam. The specific

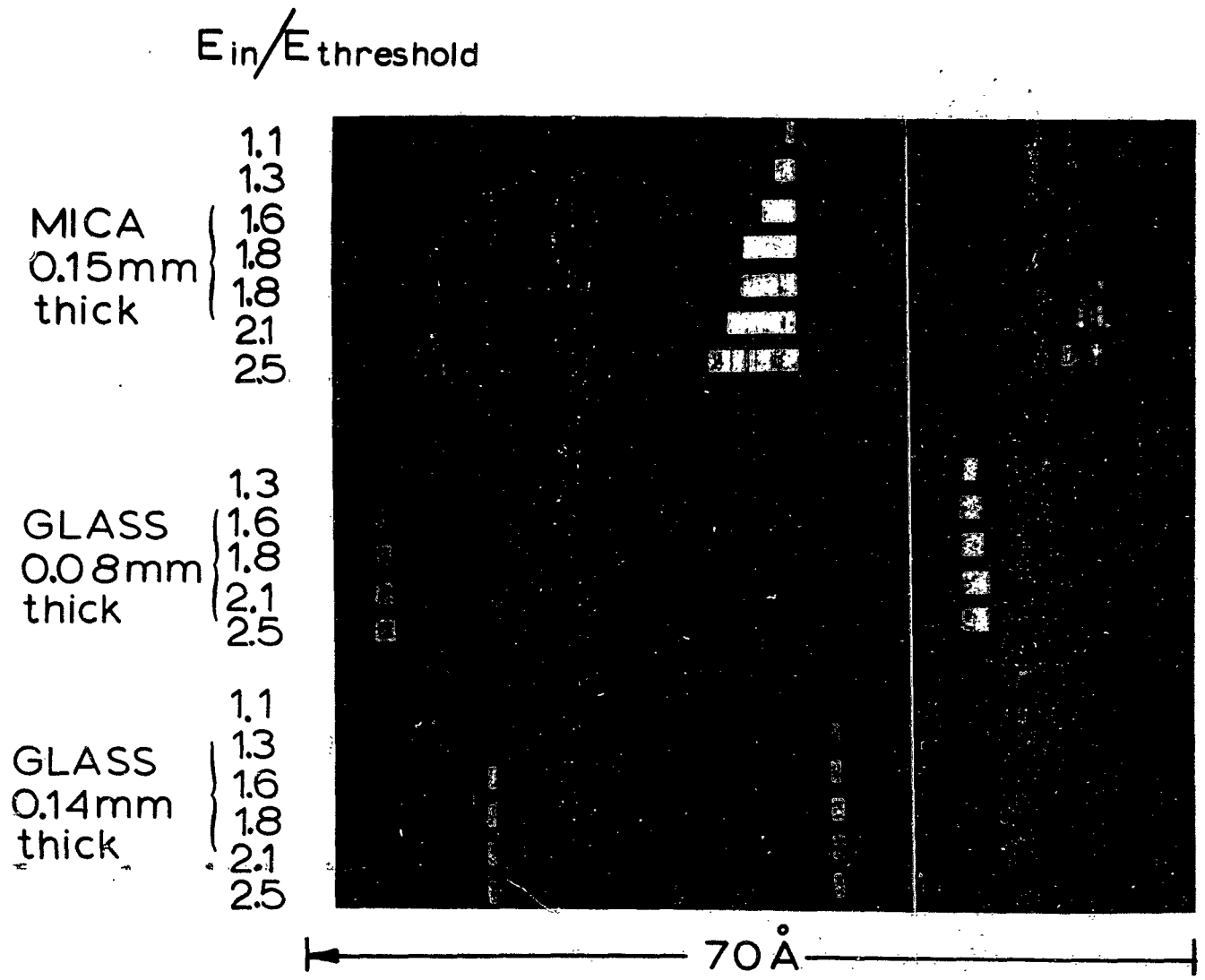

FIGURE 4. Spectra at various pump powers and plate thicknesses of glass and mica plates with a narrow beam, unclad laser rod.

heat of mica is 0.86J/g°C and its density is 2.9g/cc. For a cross-sectional area of 0.3 cm^2 the volume is approximately 0.5×10^{-2} cc and the temperature rise per joule absorbed is approximately 90°C/J. For the experimental arrangement used the threshold was 210 J electrical energy into the flashtube with a conversion efficiency above threshold of 4.2%. The data shown for 2.5 times threshold gave an output of 13 joules. The temperature rise expected is then 51°C. The agreement with the measured value of 58°C is satisfactory.

In Fig. 5 are given the spectra when an aligned plate and a tilted one are used. The separation between plates was 5 cm and the distance from the end of the laser to the tilted plate was 6 cm. The aligned plate P_1 was 0.65 mm thick and the tilted plate P_2 was 0.11 mm. Both were made of glass. The laser was unclad and emitted in a beam of less than 1° in all cases. The spectra were obtained as a function of the angle θ of tilt of the canted plate. As θ increases the thickness of plate presented to the beam changes and the wavelength shifts accordingly. The apparent thickness change follows $\cos^{-1}\theta$, which is in rough agreement with the spectra shown.

When $\theta = 0$, the plate P_2 in Fig. 5 acts as a reflection filter. There is an abrupt shift in wavelength because the resonant condition has changed from wavelengths at which the plate thickness is an even number of $\lambda/4$ to that at which the plate is an odd number. Furthermore, the spectrum has many more lines over a wider wavelength interval. This probably results from a coherent combination of reflectivities from

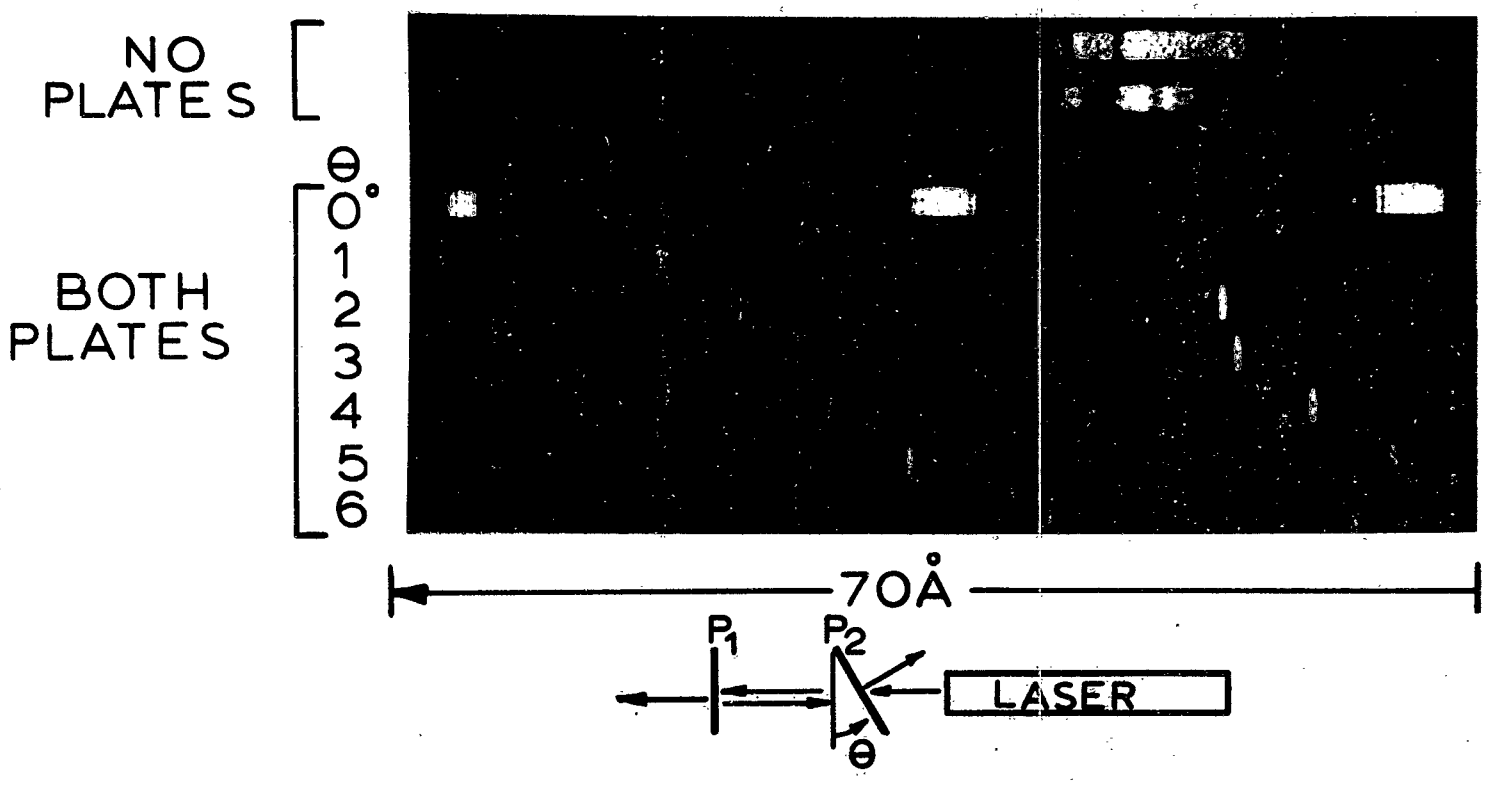

FIGURE 5. Laser spectra for an aligned and a tilted plate. The tilted plate P_2 was 0.11mm thick glass and 6cm from the rod. The aligned plate P_1 was 0.65mm thick glass and 5cm from P_2.

the plates and the end of the laser rod. During the process of lasing the spacing between rod and plate could change which would create sufficient instability to cause mode hopping.

In Fig. 6 is shown schematically a Q-switched laser which uses a rotating prism. The laser spectrum consists of a series of sharp lines that correspond to the channel spectrum for a plate whose thickness is 2d with d as the distance from the apex of the prism to the base of the prism. Occasionally the spectrum shows every other line suppressed as in the lower frame in Fig. 6. This is probably due to a subsidiary condition introduced into the possible standing waves that can exist in the prism by an imperfect apex.

In another experiment with a Q-switched laser, a laser rod was used with both ends cut at Brewster's angle. The resonant cavity had a rotating prism opposite one end of the rod and at the other end a thin plate whose channel spectrum consisted of lines 8A apart. The spectrum produced was essentially the same as that obtained without Q-switching by keeping the prism stationary.

A clad rod with a wide beam spread has a damped oscillation for a time trace as shown in the upper frame of Fig. 7. With the introduction of a thin reflecting plate aligned parallel to the exit surface of the laser rod and 4 cm from it, the time trace shows spikes as in the bottom frame of Fig. 6. Since spikes in the time trace are associated with narrow spectral lines in the laser spectrum, it is not surprising that the mode selection provided by the reflecting plate would not

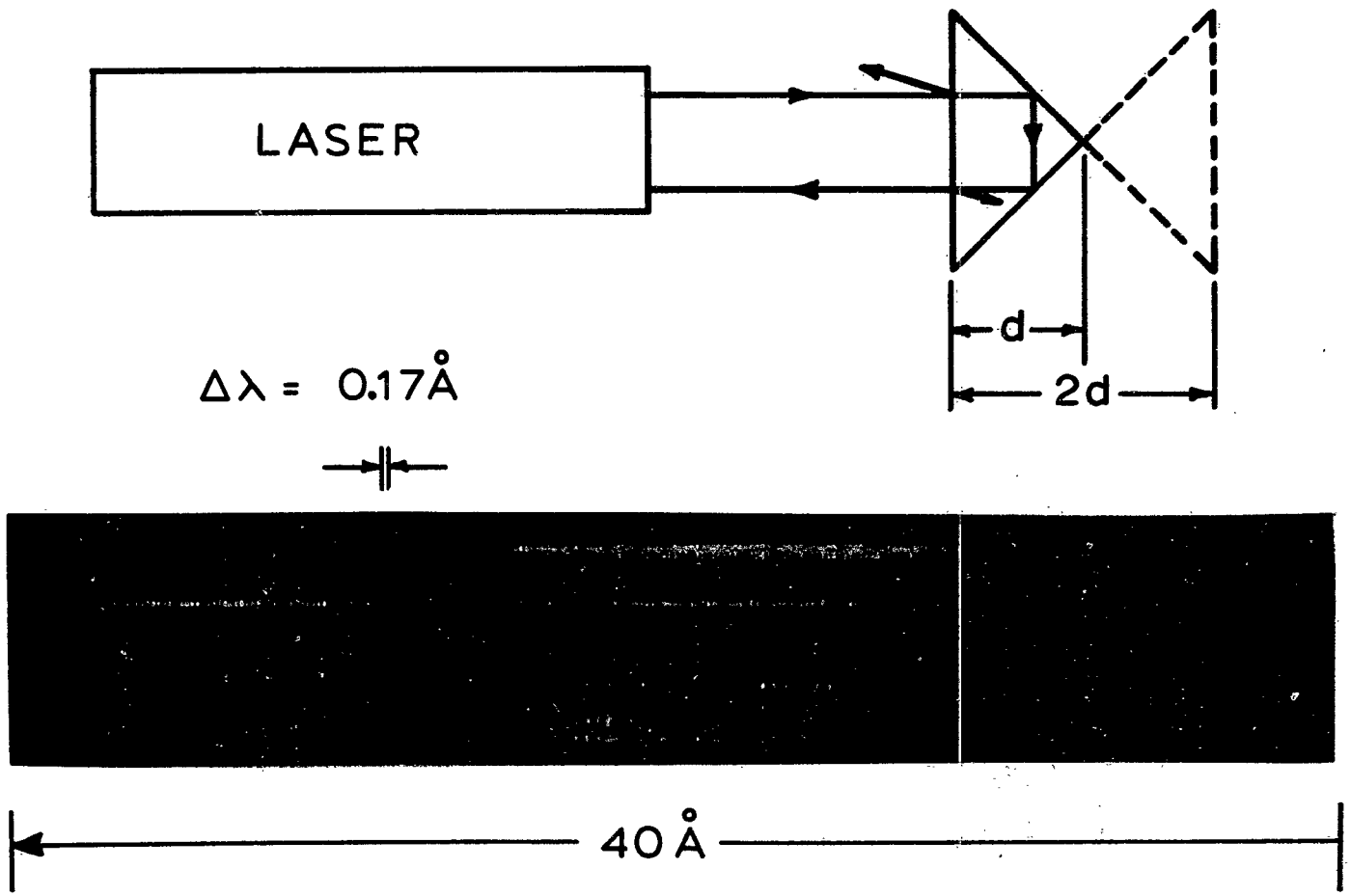

FIGURE 6. Spectra obtained from a Q-switched laser using a rotating prism. The prism behaves like a tilted plate with a thickness 2d, where d is the height of the prism.

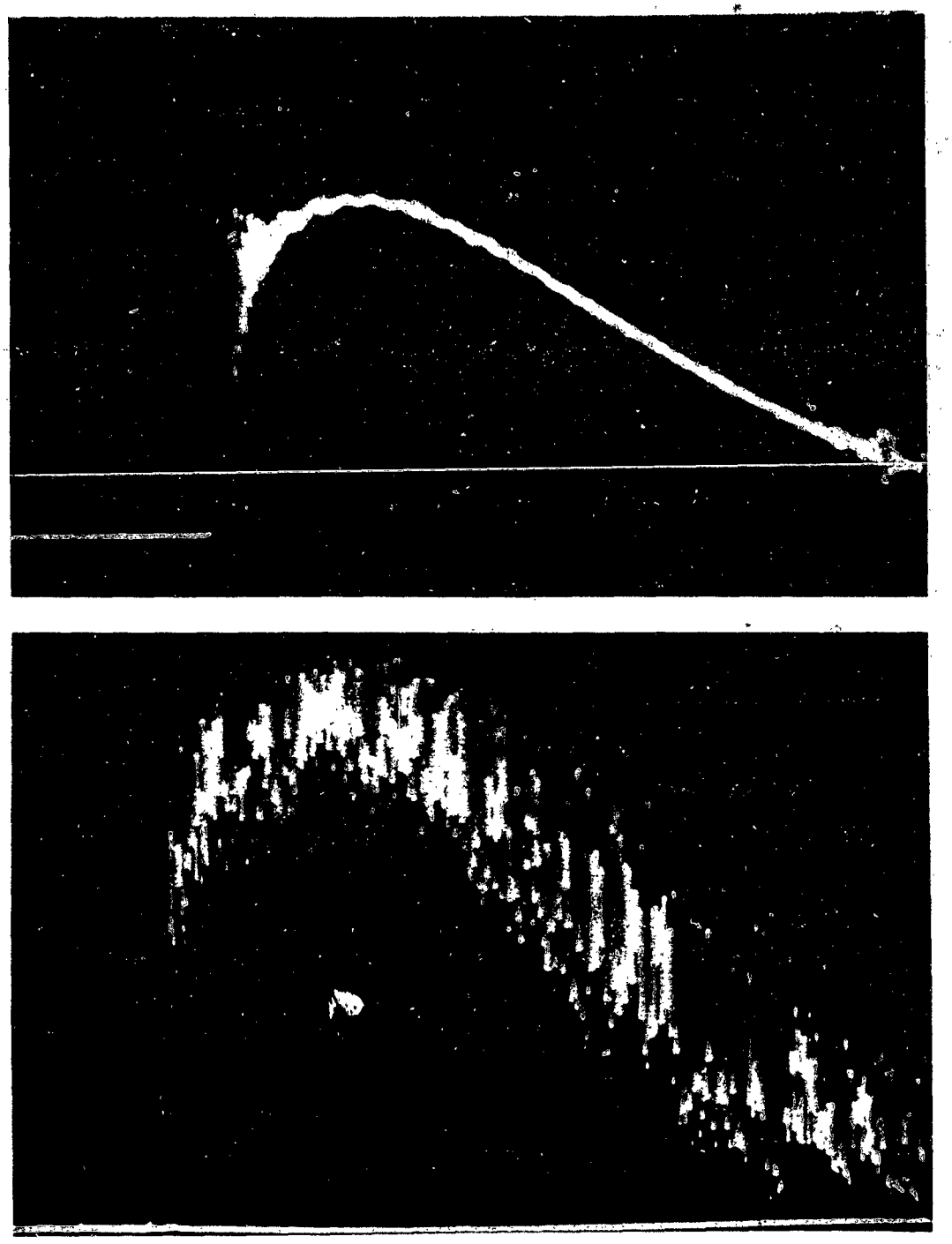

FIGURE 7. Time traces with and without an aligned reflecting plate for a clad rod. The plate produces a spiking behavior. Both traces were taken with the laser pumped at five times the threshold for the case without the plate.

only give narrow spectral lines but also produce a spiking time trace. Narrow beam lasers which would normally emit in sharp spectral lines with spikes in the time trace did not show any change in the time trace with the introduction of a reflecting plate.

The use of thin reflecting plates does not lower the output of the laser. The higher reflectivity at the laser wavelengths provided by the reflecting plate decreases the threshold, in some cases by as much as a factor of 2 by use of a plate with surface reflectivities of only 0.04. The slope of laser light-out vs. pump power is usually lowered slightly, probably due to greater losses by absorption in the cavity. However, in all cases, with an aligned plate, the laser light output increased with the use of a glass plate with a surface reflectivity of 0.04. The reduction in threshold is shown in Fig. 7 by the earlier onset of laser oscillations for the case with the reflecting plate.

By changing the temperature of the plate it is possible to determine the total change in optical path length with temperature of the material from which the plate is made. In Fig. 8 are shown the spectra obtained for a glass plate which is typical of the glasses used in lasers. By an independent measurement of the expansion coefficient it is possible to measure the thermal coefficient of the index of refraction. Values for this coefficient have been found for different glasses that vary from -37×10^{-7} up to $+45 \times 10^{-7}/^{\circ}C$.

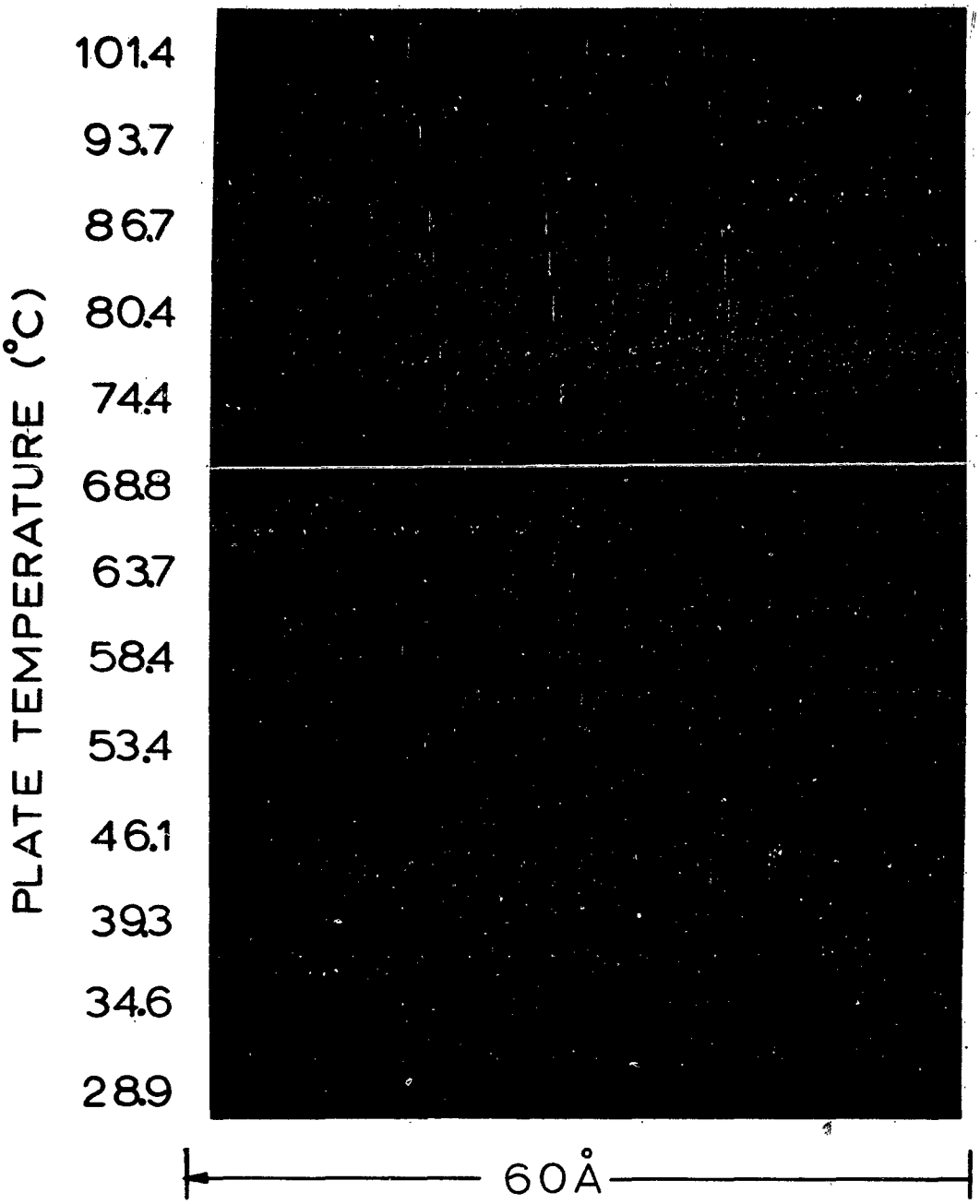

FIGURE 8. Laser spectra as a function of glass plate temperature.

III. Nd^{3+} LINE BROADENING IN GLASS

A. Review of Non-laser Spectroscopic Data

In Fig. 9 is shown the absorption spectrum for a 6.4mm thick sample of a glass with the composition 66 wt.% SiO_2, 5 wt.% Nd_2O_3, 16 wt.% K_2O, 5 wt.% Na_2O, 5 wt.% BaO, 2 wt.% Al_2O_3, and 1 wt.% Sb_2O_3. Absorption in any of the levels shown leads to fluorescence with nearly 100% quantum efficiency from the $^4F_{3/2}$ state, which appears as the absorption at 880mμ.

The spectra for alkali, alkali earth, silicates are very similar to one another. To see the details of the structure in the levels involved in laser emission, the composition 71.5 wt.% SiO_2, 2.5 wt.% Nd_2O_3, 10 wt.% K_2O, 10 wt.% Rb_2O, 5 wt.% BaO, and 1 wt.% Sb_2O_3 was used because it gave relatively narrow lines. The absorption and fluorescent spectra involving the $^4F_{3/2}$ state for this composition at room temperature and at 77°K are shown in Fig. 10. The fluorescent laser line at 1.06μ is shown for the same glass in Fig. 11. The curves in Figs. 10 and 11 were taken on a Cary Model 14 Spectrophotometer with the slits set for a resolution of 10A. From the absorption and fluorescence data, the energy level diagram in Fig. 12 can be obtained. Other alkali, alkali earth, silicates give essentially the energy level diagram except that the ground state splitting may not be as much. The two lowest levels of the $^4I_{9/2}$ state appear as one level in a Na, Ca, silicate glass.[5]

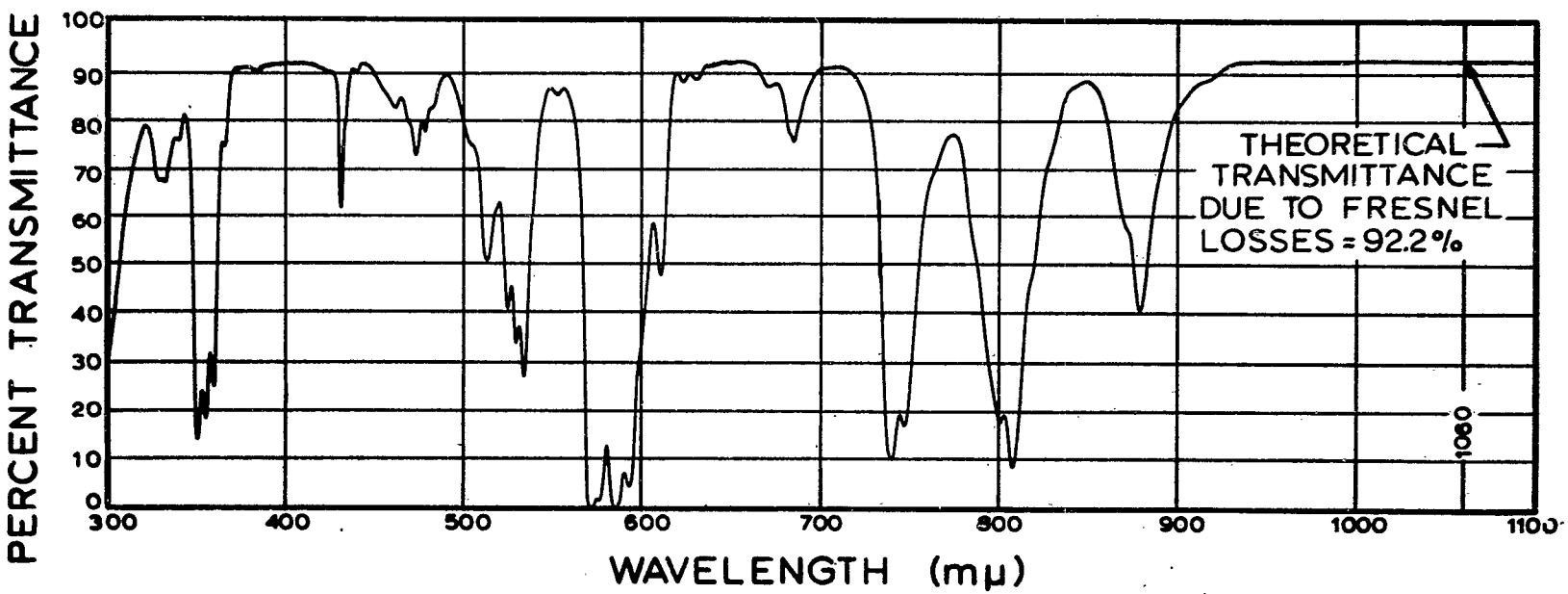

FIGURE 9. Nd^{3+} absorption spectrum for a 6.4mm thick sample of a glass with the composition 66 wt.% SiO_2, 5 wt.% Nd_2O_3, 16 wt.% Na_2O, 5 wt.% BaO, 2 wt.% Al_2O_3 and 1 wt.% Sb_2O_3.

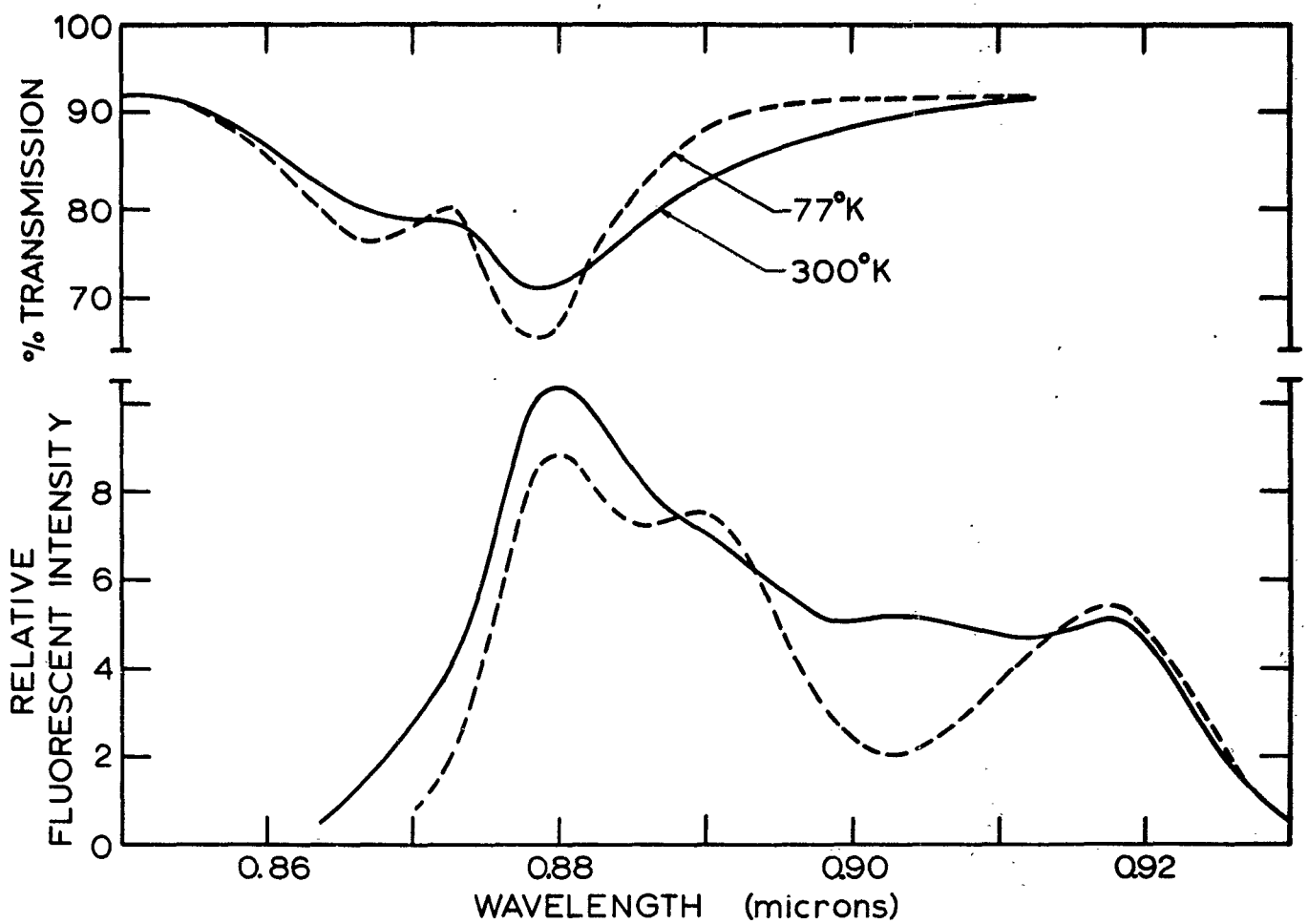

FIGURE 10. Absorption and fluorescence in 0.88μ line of Nd^{3+} in a glass with the composition 71.5 wt.% SiO_2, 2.5 wt.% Nd_2O_3, 10 wt.% K_2O, 10 wt.% Rb_2O, 5 wt.% BaO, and 1 wt.% Sb_2O_3.

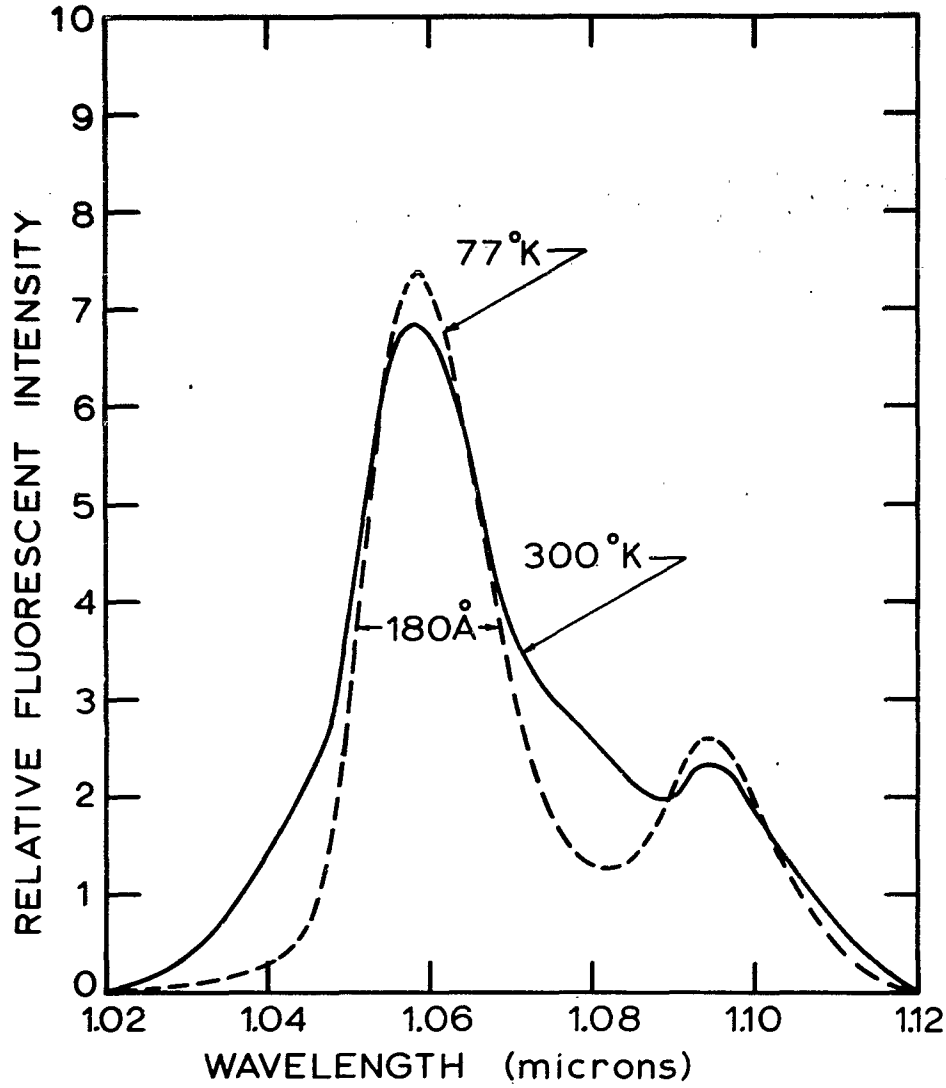

FIGURE 11. Fluorescent emission of the 1.06μ line at 300°K and 77°K for Nd^{3+} in a Rb-K-Ba silicate glass.

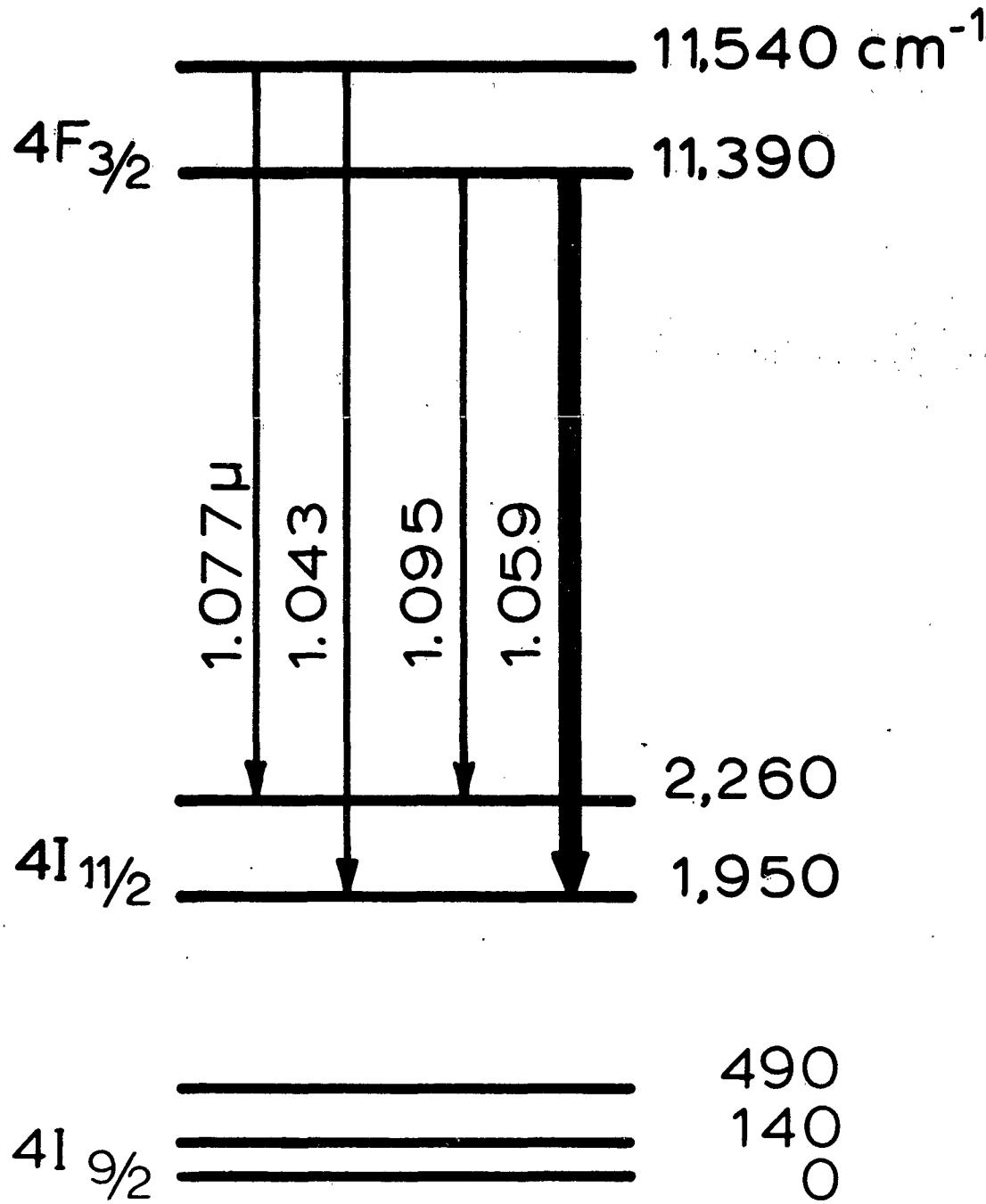

FIGURE 12. Energy level diagram for the ground state and the states involved in laser emission at 1.06μ for Nd^{3+} in a Rb-K-Ba silicate glass.

The splitting of the ground state is of importance in increasing the pumping at room temperature. At 300°K, there is sufficient population in the upper of the split $^4I_{9/2}$ state to provide additional absorption bands approximately $450cm^{-1}$ to the long wavelength side of existing bands. This is shown by the absorption to the $^4G_{5/2}$ and $^2G_{7/2}$ states at 300°K and 77°K in Fig. 13 for the Rb silicate.

In Fig. 14 are shown the intensity of fluorescence at 300°K following a 10μsec pump pulse of light for four concentrations of Nd_2O_3 in a glass base with the composition 59 wt.% SiO_2, 25. wt.% BaO, 15 wt.% K_2O, and 1 wt.% Sb_2O_3. The sample with 0.5 wt.% Nd_2O_3 has an initial decay time of 0.55msec, which increases to 0.90msec after 3msec. At lower concentrations, the same values are obtained. For concentrations greater than 1 wt.%, the curves show concentration quenching by the decrease in the slopes. The mechanism proposed by Petersen and Bridenbaugh[6] for concentration quenching of Nd^{3+} in $CaWO_4$ probably operates in the glass as well. An excited Nd^{3+} ion can interact with an unexcited neighbor by making the transition from the $^4F_{3/2}$ state to $^4I_{15/2}$ and the neighboring ion makes the transition $^4I_{9/2} \rightarrow {}^4I_{15/2}$. Then both decay nonradiatively back down to the ground state. The quenching process is shown by the dotted lines in the insert in Fig. 14.

When interaction takes place between ions there is also the process indicated by the solid arrows in the insert in Fig. 14, All the energy is transferred between neighbors. Neighboring sites are not

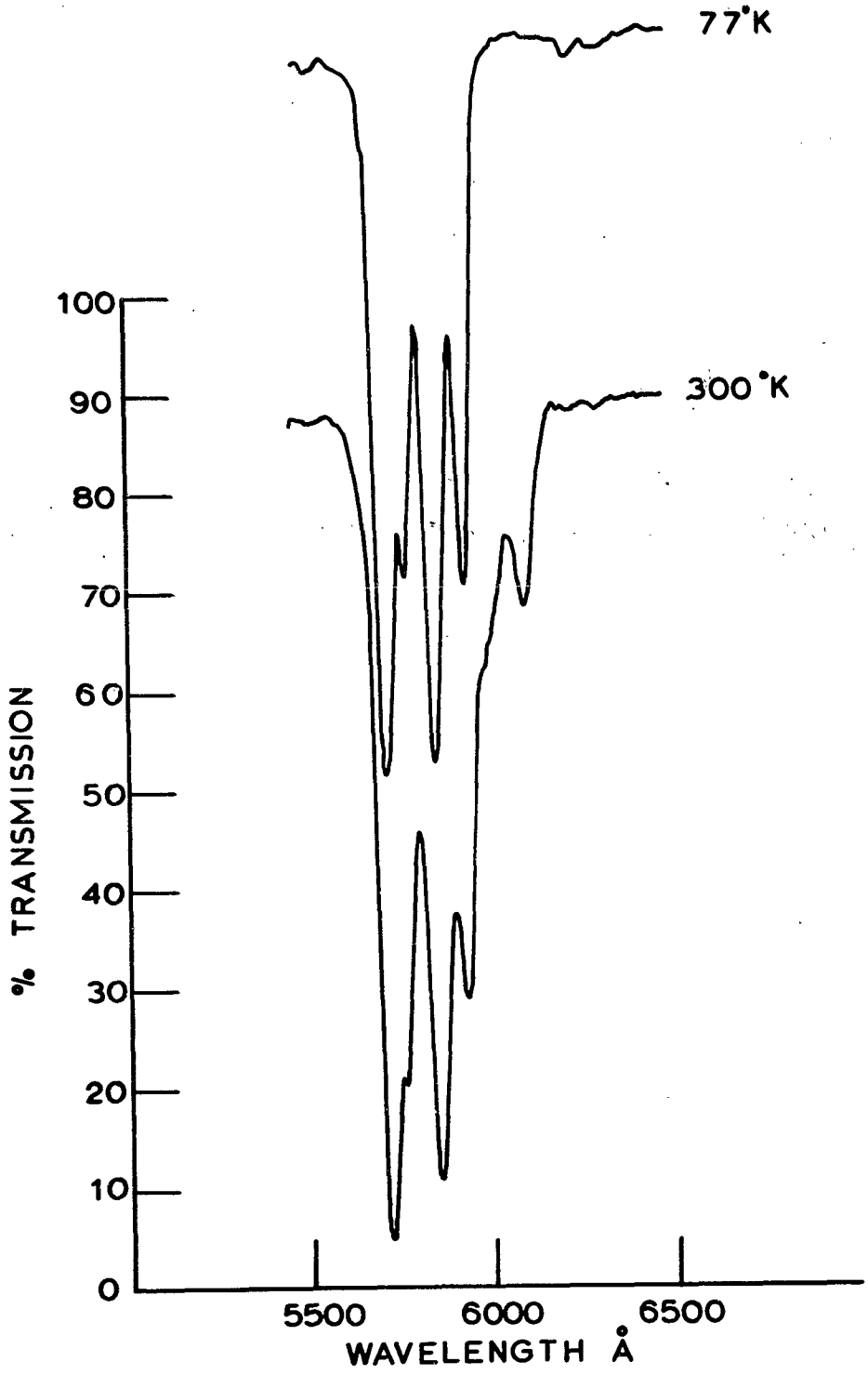

FIGURE 13. The absorption to the $^4G_{5/2}$ and $^2G_{7/2}$ states at room temperature and 77°KK This illustrates the increased pumping provided by thermal population in the upper of the split $^4I_{9/2}$ ground state for alkali, alkali earth, silicates.

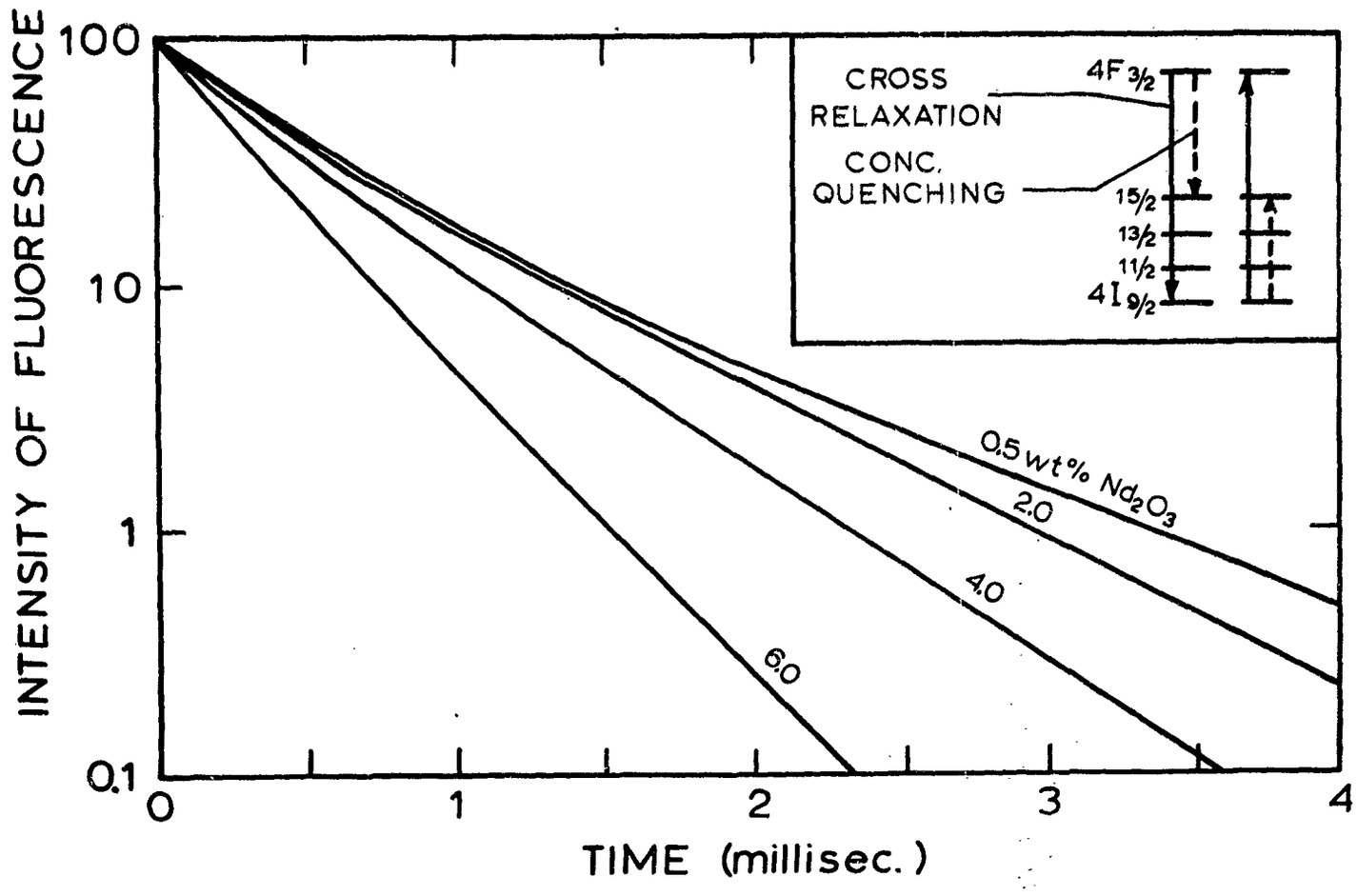

FIGURE 14. Fluorescent intensity as a function of time following a 10μsec pump pulse for various concentrations of Nd^{3+}. The insert shows the cross relaxation and quenching mechanisms, which respectively, tend to make the lines straighter and to increase the slope.

likely to be exactly the same. The differences in ligand field lead to a shift in energy across the line which contributes a cross relaxation process when hole burning occurs in laser emission. The concentration quenching decreases the lifetime for fluorescence and the cross relaxation smooths out its time dependence so that it tends to follow more nearly a simple exponential. For example, the sample with 6 wt.% Nd_2O_3 has an initial decay time of 0.31msec and a value after 3msec of 0.36msec. The quenching is a function of the spacing between ions. Since the ions are randomly distributed there is a distribution of spacing. The net result is a tendency to have a time dependent lifetime even though cross relaxation tends to smooth out its time dependence. An accurate assessment of the cross relaxation rate as a function of concentration from this data is difficult.

Maurer has fitted the data for Nd^{3+} in a Na-Ca-Si glass to a sum of exponentials and found that the spread in transition probabilities was about as wide as the mean value.[5] To take account of cross relaxation would require the further complication of the random distribution of the ions in the glass. From the curves, a reasonable conclusion is that the quenching and the cross relaxation rates are about the same.

In quoting lifetime data either the intitial lifetime can be given or some convenient arbitrary convention established, such as the equivalent exponential lifetime that goes through the 70% and 30% points. The latter was used here. Fortunately, the curves are near enough to

an exponential in this limited region that the results are almost identical.

The longest lifetimes of Nd^{3+} fluorescence are found in alkali, alkali earth, silicates. Values as long as 1msec can be obtained for Rb-Ba-Si glass.[7] The borates have τ values less than 100μsec. By comparing the peak absorption in the $^4I_{9/2} \rightarrow {}^4F_{3/2}$ transition to the inverse of the lifetime for several glasses, Harper concluded that the differences in lifetime were due in part to differences in the matrix elements for radiation and in part to changes in the radiation less transition probabilities from the $^4F_{3/2}$ level.[10]

For silicate glasses with concentrations low enough so that concentration quenching does not occur, the lifetime was found to decrease with a decrease in temperature.[11] This is due to a smaller thermal population in the upper of the split $^4F_{3/2}$ state. From the absorption spectrum, the transition probability to ground is less for the upper than for the lower of the $^4F_{3/2}$ state. Depending on the composition, the annealing of the glass could either increase (by as much as 20%) or decrease the lifetime.[12]

The change in lifetime with concentration for two glass series is shown in Fig. 15. The glasses with the larger alkali ions not only have a longer lifetime, but the concentration obtainable before significant concentration quenching occurs is also greater. This is to be expected on the model for quenching proposed by Petersen and Bridenbaugh if the ion interactions are dipole in character. From

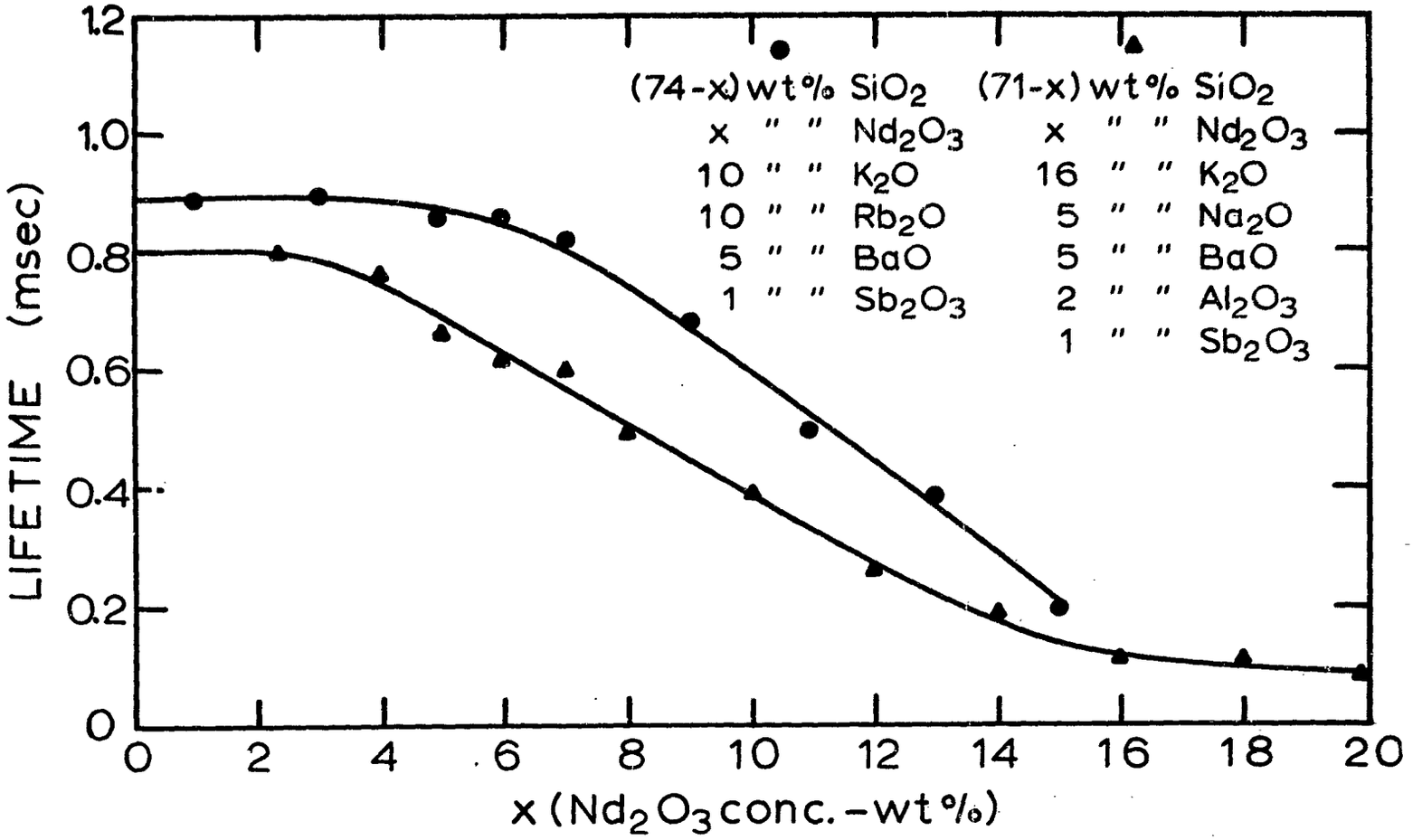

FIGURE 15. The lifetimes as functions of concentration for two glass series.

the relatively constant ratios of the intensities of the 0.88μ, 1.06μ and 1.35μ fluorescent lines in various alkali, alkali earth silicates, the ratios of two matrix elements from the $^4F_{3/2}$ state to lower states are independent of the host. Equivalent dipole matrix elements contribute to the radiative emission rate and the dipole-dipole interaction.

For high concentrations, the lifetime falls off less rapidly than linear. This may in part be due to the increased quenching for the ions that interact strongly, with the result that the relatively more isolated ions contribute more to the measured lifetime.

B. Laser Emission vs. Time

In Fig. 16 are shown three typical time traces for laser output light. Fig. 16A is the characteristic random spiking from either clad or unclad rods which have narrow beam spreads. Here well defined standing waves are established in the resonator, but due to thermal effects and microphonics the conditions for high Q modes are irratically established. The result is multi-moding and random spiking in the time trace.

In Fig. 16C is the typical behavior of a clad rod with a good interface between core and cladding and a lower refractive index for the cladding so as to provide a large number of modes of equal Q by total internal reflection. If the Q's are made relatively low by use of a low end reflectivity and if striated neodymium glass is used so

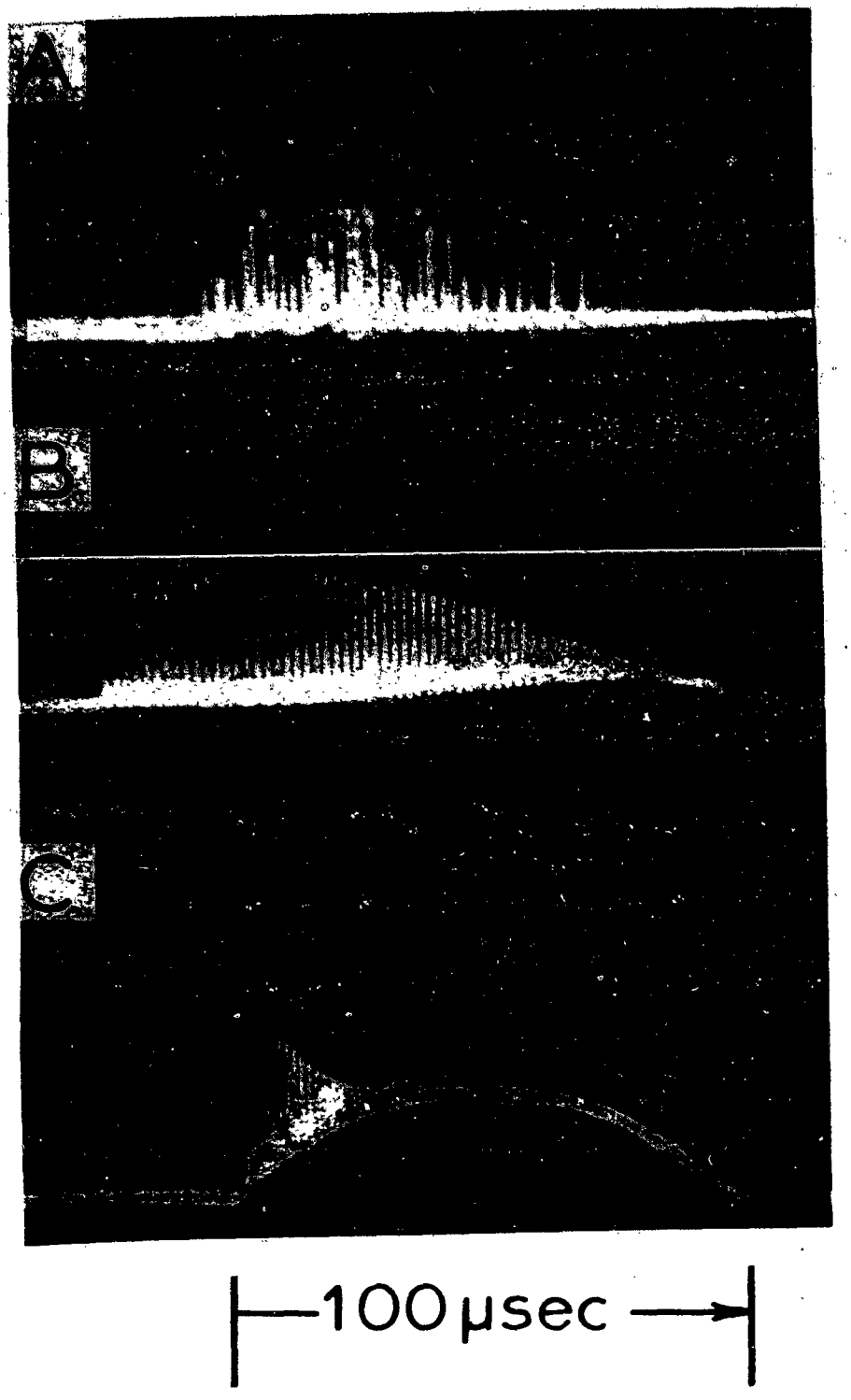

FIGURE 16. Typical time traces for laser emission.
A. Random spiking in an unclad rod.
B. Limit cycles in a clad rod.
C. Damped oscillations in a clad rod.

that standing waves between the end reflectors are not established, the system responds as a single unit. The picture shown was taken 50% above threshold on a 50cm long rod, 0.6cm core diameter, and 0.9cm O.D. for the clear cladding. The ends were flat and parallel with an opaque silver reflector evaporated on one end and only the 4% Fresnel reflection for a glass-air interface at the exit end. The indices of refraction for the core and cladding were 1.53 and 1.52. Even if the index of refraction of the cladding is greater than the core, a strongly damped oscillation such as Fig. 16C can still be obtained. Fresnel reflection at grazing incidence is enough to confine the light. The essential requirement is that there not be isolated standing waves established in the resonator. The beam spreads obtained are 8° or larger and there is not interference or structure in the radiation pattern. The spectrum consists of bands a few angstroms wide instead of the sharp lines characteristic of isolated high Q modes that gives the time traces of Fig. 16A.

In Fig. 16B is shown an undamped train of relaxation oscillations obtained from a clad rod which was only slightly striated and in which the cladding index was larger than the core index of refraction. The beam spread was 4°, without any structure in the radiation pattern, and the spectrum was in the form of bands rather than sharp lines. The cause of undamped oscillations, or limit cycles, is still unclear for glass with Nd^{3+} as the only colorant. The conditions under which Fig. 16B was obtained are more nearly like those that produced 16C

than 16A, except that the beam spreads are narrower than for 16C. It will be shown presently that whatever the mechanism is that gives limit cycles, they are favored when the beam spread is narrow.

The rate equations have been used by Statz and de Mars[13] to explain the relaxation oscillations in the transient response of masers. The rate equations can easily be generalized to include the influrence on the damped oscillations caused by cladding the laser rod and by high Nd^{3+} concentration effects, such as concentration quenching and cross relaxation. The coupled non-linear equations that give the number of photons per unit volume J in the cavity and the inverted population per unit volume N are

$$\frac{dJ}{dt} = -LJ + (Af + BJ)N \tag{9}$$

$$\frac{dN}{dt} = P_o - (Ah_o + BJ)N + C(N' - N) \tag{10}$$

The time constant 1/L for the cavity is related to the Q by

$$L = 2\pi\nu/Q \tag{11}$$

The spontaneous emission term AfN in Eq. (9) involves the product of the Einstein A coefficient and the factor f which gives the fraction of spontaneously emitted light that is coupled into the finite numerical aperture of the clad rod. For core and cladding indices n_1 and n_2, it is

$$f = (n_1 - n_2)/n_2 \tag{12}$$

The factor h_o takes account of other processes that deplete the inversion, such as spontaneous emission in other lines and non-radiative transitions. It is related to the measured lifetime τ_m by

$$Ah_o = 1/\tau_m \tag{13}$$

The cross relaxation term is proportional to a rate constant C and the difference in population between the actual inversion N and the inversion N' that would exist if no laser light were present in the cavity. The value of N' is proportional to the pump power P_o. Since cross relaxation drops out for an optically thin sample,

$$N' = P_o/Ah_o \tag{14}$$

The cross relaxation term can be incorporated into the other terms by redefining the coefficients P and h by

$$P = P_o(1 + C/Ah_o) \tag{15}$$

$$h = h_o + C/A \tag{16}$$

A set of coupled nonlinear equations such as Eqs. (9) and (10) have been discussed by several authors.[13-16] The procedure for illucidating the oscillatory behavior is straightforward. First, the steady state values J_o and N_o are found at which $dJ/dt = dN/dt = 0$. The equations are then considered for small oscillations about the steady state value. Make the substitutions

$$J = J_o + j(t),$$

$$N = N_0 + n(t) \tag{17}$$

Eqs. (9) and (10) can be linearized for their dependence on $j(t)$ and $n(t)$. A single equation can be obtained for $j(t)$, which is

$$\frac{d^2 j}{dt^2} + \frac{2}{T}\frac{dj}{dt} + (\omega^2 + \frac{1}{T^2})j = 0 \tag{18}$$

The solution is

$$j = \text{const.} \exp\left\{-t/T\right\} \cos \omega t. \tag{19}$$

Because of the term AfN in Eq. (9), there is not a precise threshold for oscillation. For convenience the threshold P_t that would exist if $f = 0$ is introduced. The pump power P can be expressed in terms of P_t by

$$P = qP_t \tag{20}$$

$$P_t = AhL/B \tag{21}$$

$$N_t = P_t/Ah \tag{22}$$

The solutions for the relevant quantities are

$$N_0 = \frac{L}{2B(1-f/h)} \left\{ (q+1) - \sqrt{(q-1)^2 + 4qf/h} \right\} \tag{23}$$

$$J_0 = \frac{Ah}{2B} \left\{ (q-1) + \sqrt{(q-1)^2 + 4qf/h} \right\} \tag{24}$$

$$2/T = qP_t/N_0 + fAN_0/J_0 \tag{25}$$

$$\omega^2 = LBJ_0 - (fAN_0/J_0 - qP_t/N_0)^2/4 \tag{26}$$

Except near threshold where Af is comparable to BI, the equations

are conveniently solved to first order in f. In this approximation the damping time τ and oscillation frequency ω reduce to

$$\frac{2}{\tau} = qAh + \frac{f}{h}\frac{1}{q-1}(L + qAh) \tag{27}$$

$$\omega^2 = (q-1)AhL\left[1 + \frac{f}{h}\frac{q}{(q-1)^2}\right] - \frac{1}{4}\left[\frac{f}{h}\frac{L}{q-1} - qAh\right]^2 \tag{28}$$

Eqs. (23) and (24) give the expected result that more light is in the cavity for a smaller inversion for $f \neq 0$ as compared with their values when $f = 0$. The damping of the relaxation oscillations with increasing concentration of Nd^{3+} in the glass would go up more rapidly than the decay constant for spontaneous emission due to the addition of the cross relaxation rate C to the inverse of the measured lifetime Ah_o.

A non-zero value of f contributes an additional term to the damping of the relaxation oscillations. An order of magnitude estimate of the factors in Eq. (27) are $Ah \cong 3 \times 10^3 sec^{-1}$, $C \cong 10^3 sec^{-1}$, $q = 2$ gives $q(Ah + R) \cong 10^4 sec^{-1}$. For the unclad rod whose time trace is shown in Fig. 10A, the term containing f can be neglected. This damping time is long enough so that microphonics and thermal distortions interrupt the train of pulses. There results in this case, a random superposition of partial trains of pulses which shows up as random spiking.

For h = 3, L = $10^9 sec^{-1}$, and q = 2, the second term in Eq. (27) predominates if f is greater than about 10^{-4}. Since typical values of f are of the order of 10^{-2}, this accounts for the smooth, strongly damped oscillation in the time traces of the clad rods.

The appearance of undamped oscillations, or limit cycles, in the relaxation oscillations of Fig. 16B is still not explained. They occurred when the beam spread was less. This is reasonable for a smaller value of f gives a narrower beam spread and less damping so that whatever the mechanism is for limit cycles it can more readily take over. As for the basic mechanism, it is uncertain. Very likely, there is a saturated absorption similar to that proposed by Shimoda[28] to explain limit cycles in ruby. To take account of a slight saturable absorption, L in Eq. (9) is replaced by $(L_o - L_1 J)$, where $L_1 J_o << L_o$. This adds the term $(-L_1 J_o)$ to the right side of Eqs. (25) and (27).

The limit cycles would be produced under high pumping conditions, as is the case. It is also found that they are favored at low temperature. This may be due to the ability to more readily saturate a transition at low temperature where nonradiative processes are less active. Exactly which transition in Nd^{3+}, or possibly an impurity, is responsible is not known. As pointed out by Shimoda, $L_1 J_o / L_o$ need only be of the order of 10^{-4}.

C. Laser Spectral Output

The spectral output was quite different for unclad rods that showed random spiking than for clad rods that gave damped oscillations.

The latter time traces produced continuous bands whereas random spiking gave sharp lines. From time resolved spectra, it was found that emission could occur in several lines simultaneously in one spike. The wavelength interval over which laser emission occurred depended on the pump power. In Fig. 17 is shown the spectral distribution of the laser output for a rod having a 1° beam spread and with random spiking in the time trace. In Fig. 18 is shown the wavelength interval, as taken from Fig. 17, over which laser emission occurs as a function of input pump power. With sufficient pumping, laser emission can be made to occur over as wide an interval as 130A. The wider emission occurs at low concentration of Nd^{3+} (less than 2 wt.% Nd_2O_3) and low temperature (77°K).

Inhomogeneous broadening of the 1.06μ line of Nd^{3+} in glass is clearly indicated from the simultaneous laser emission over so broad a wavelength interval. Time resolved spectroscopy shows that hole burning within the inhomogeneously broadened line also occurs.[1,17]

To investigate hole burning and related phenomena, it is necessary to avoid the dependence on high Q modes which characterizes the random spiking behavior. If clad rods are made from striated glass and with relatively low Q's due to the low end reflectivity, standing waves between the end reflectors are not established. Instead, the light output is in the form of spectral bands and is determined only by the emission characteristics of Nd^{3+} in glass. The time resolved spectra of such a clad rod are shown in Fig. 19 for 50% and 100% above

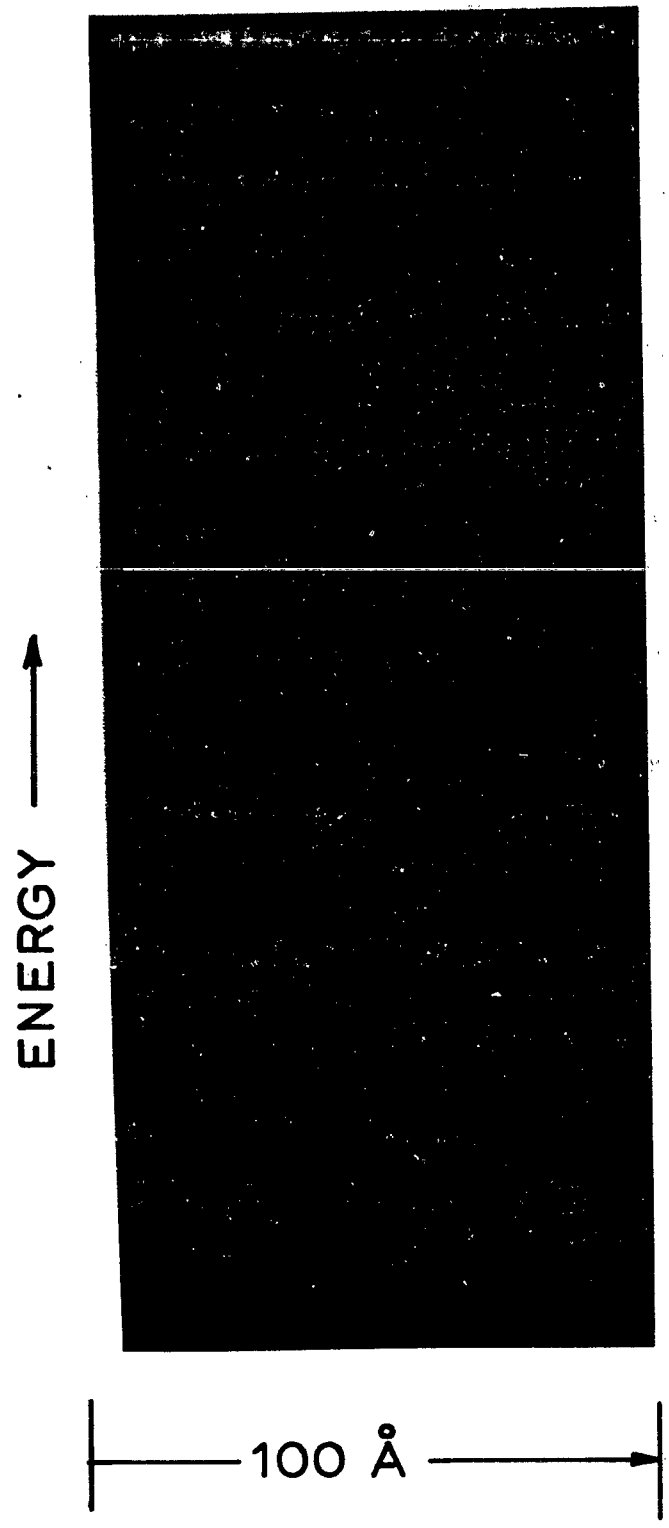

FIGURE 17. Sharp line spectra of a narrow beam laser for increasing pump power.

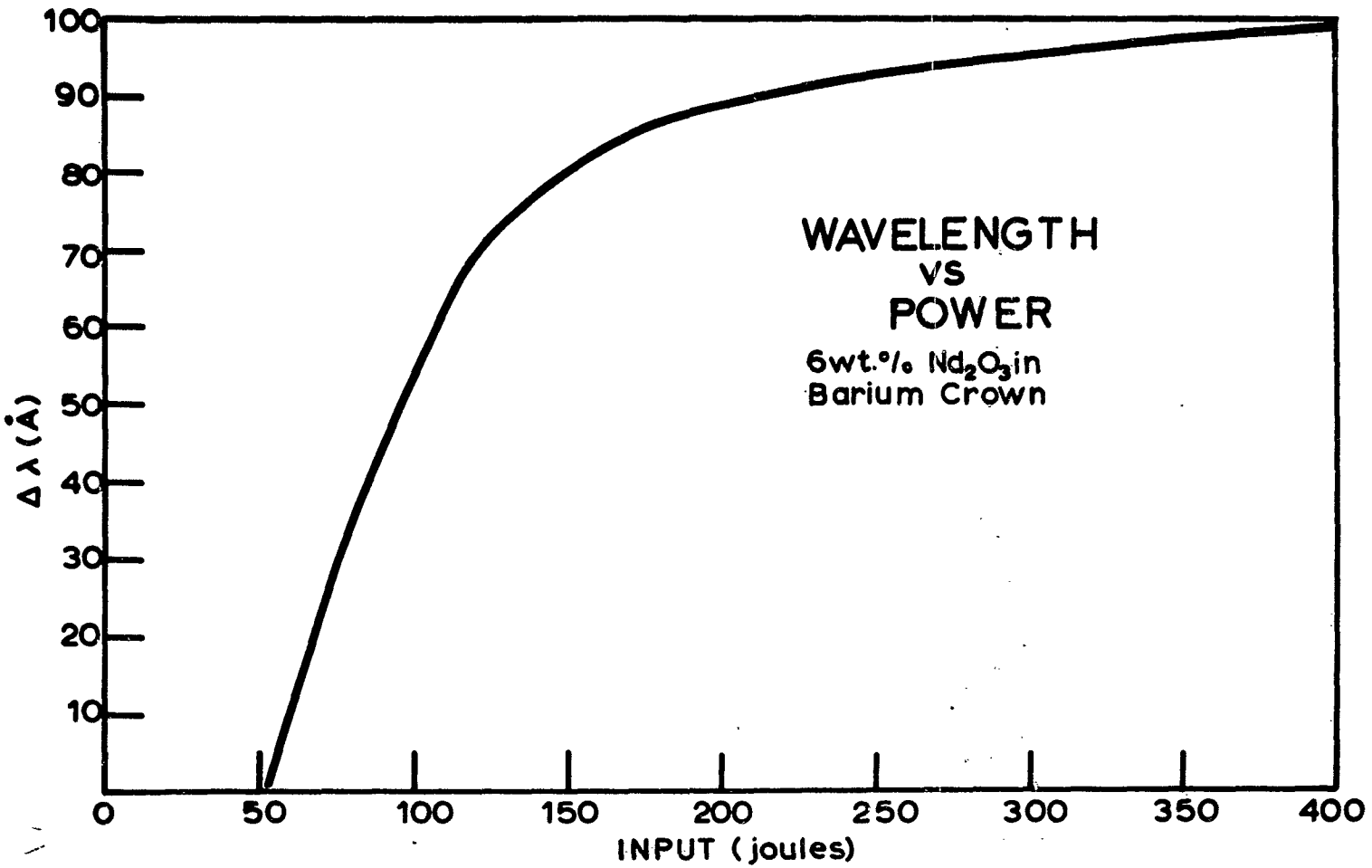

FIGURE 18. Wavelength interval $\Delta\lambda$ over which laser emission occurs as a function of pump power. Data taken at 300°K for glass with 6 wt.% Nd_2O_3.

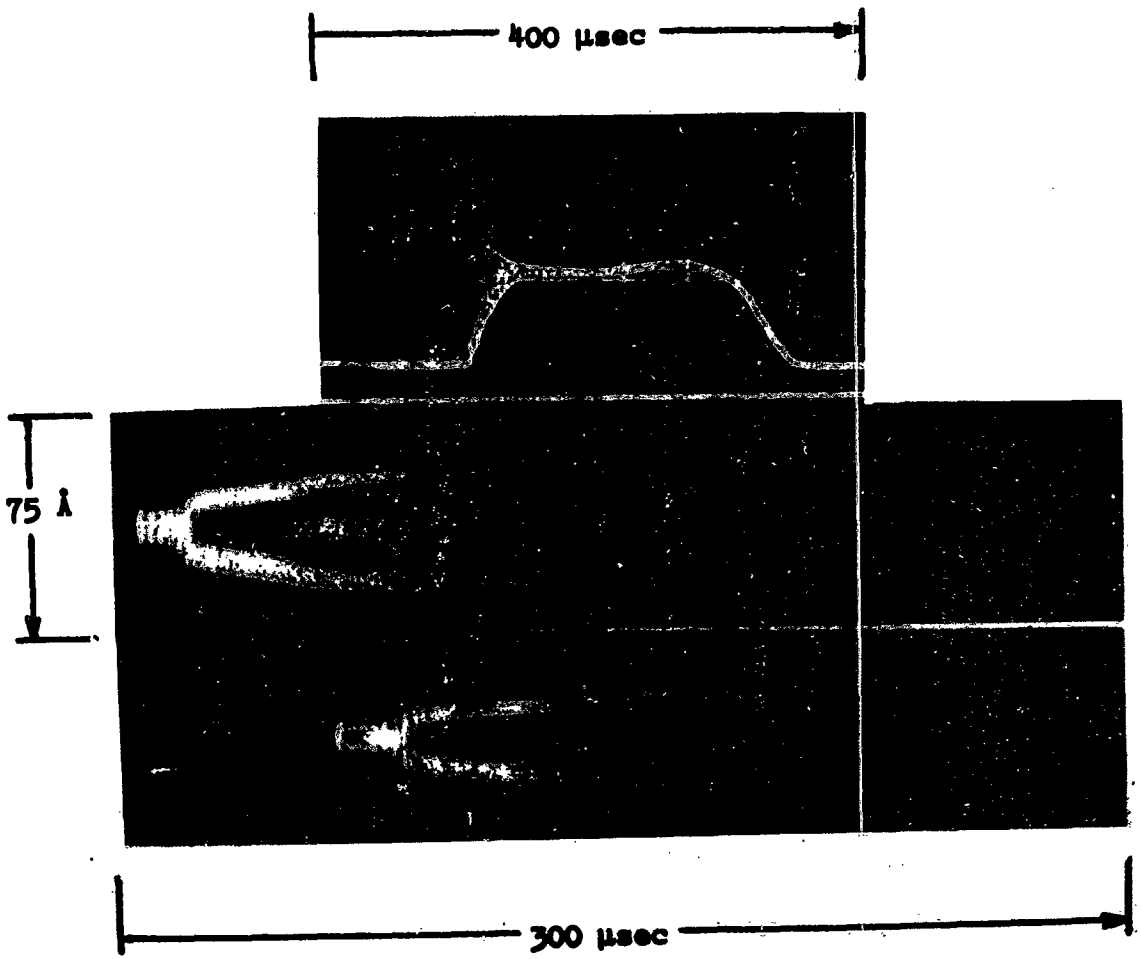

FIGURE 19. Time resolved spectra 50% and 100% above threshold of a clad rod. The time trace is for the higher pumping.

threshold. For this and the other rods used for taking the time resolved spectra the rod dimensions are 50cm long, 0.6cm laser glass with a clear cladding fused on that brought the O.D. to 0.9cm. One end had an opaque evaporated silver reflector and the exit end only the 4% Fresnel reflection for a glass-air interface. Increasing time is in the direction of the arrows. The spectra were obtained by use of a streak camera at the exit plane of a Jarrell-Ash Model 70-000, 3.4 meter, Ebert mount spectrograph. The time trace is for the higher pump power and was obtained by monitoring the back reflected light from the entrance slit of the spectrograph with an RCA 7102 photomultiplier tube.

In Fig. 20 are shown the time resolved spectra and time traces as functions of temperature for pumping 50% above the room temperature threshold. The time traces are for the lower, center and upper frames. The upper spectrum was taken at 77°K. While the rod warmed to room temperature, the other spectra were obtained.

No significant change in the hole burning was shown at room temperature when the concentration of neodymium in the glass was varied from 0.1 to 20 weight percent. There was a narrowing of the wavelength interval over which laser action occurred for the high concentrations. In the glass used concentration quenching begins at about 4 wt.%. The narrowing of the laser emission may be due to the inability to pump the rod as hard since the threshold increases above about 8 wt.%. At 77°K, emission occurred over as wide a wavelength interval for the high

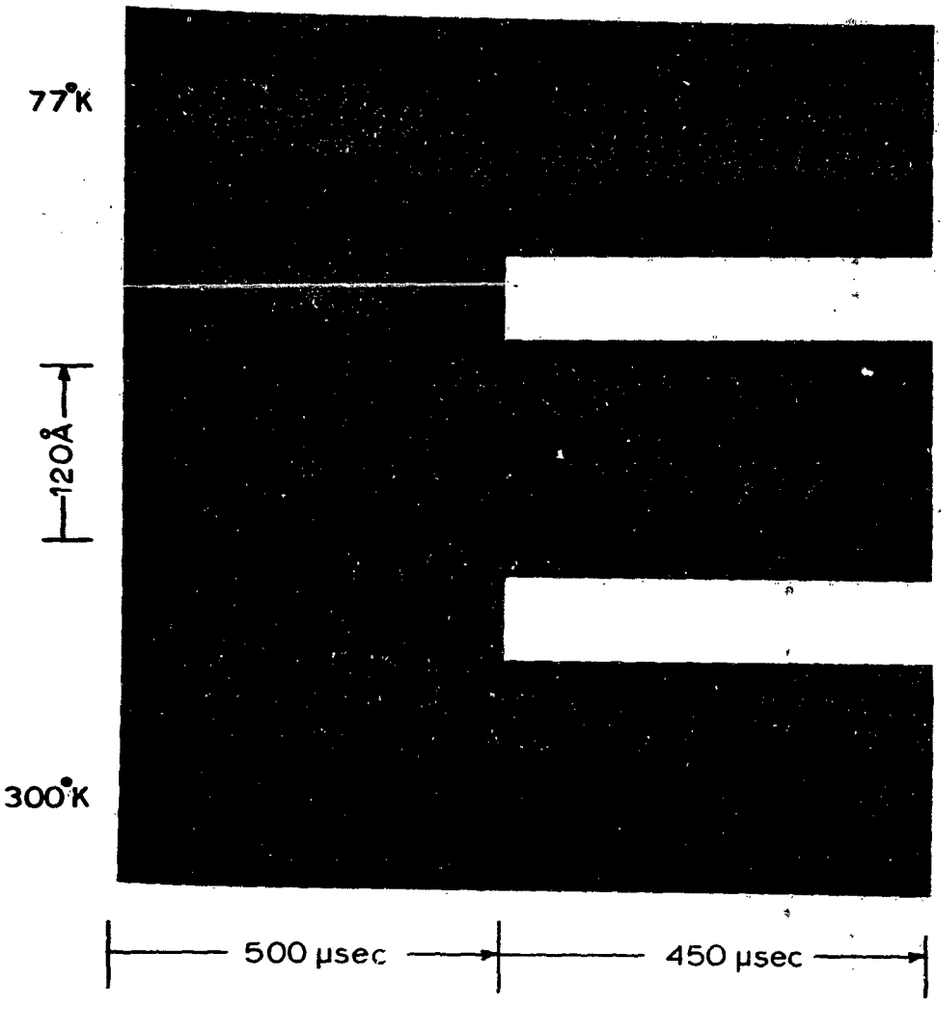

FIGURE 20. Time resolved spectra and time traces as a function of temperature of the laser for a pump power 50% above the room temperature threshold.

concentration as for the low concentration glass.

Another set of rods were made with an index of refraccion for the neodymium core glass of 1.50 and cladding glass with an index of 1.52. Some spiking occurred with a corresponding spectral emission in sharp lines, but most of the light was emitted in broad bands similar to the spectra already discussed. The Fresnel reflection for grazing incidence at the core-cladding interface provides sufficient reflectivity to contain the light. In addition, the glass was relatively striated. This tended to inhibit the establishment of standing waves between the end reflectors. The stria together with microphonics and thermal changes during pumping, made the rod behave as a single unit. The behavior of these rods was the same as those previously tested except for the low concentration glasses operated at low temperature (77° to 195°K). In the latter case limit cycles in the relaxation oscillations occurred. A spectrum and time trace are shown in Fig. 21 for a 0.5 wt.% Nd_2O_3 glass at 195°K. The alternation in intensity of every other spike in the time trace has been observed in a number of different rods. Usually it lasts for only a few spikes. Whenever these subharmonics occur in the oscillations they are always associated with laser emission occurring in alternate regions of the spectrum.

The properties of the 1.06μ line can be studied further by the use of a thin reflecting plate which acts as a frequency selective end reflector. As discussed in section II, the total reflectivity at the

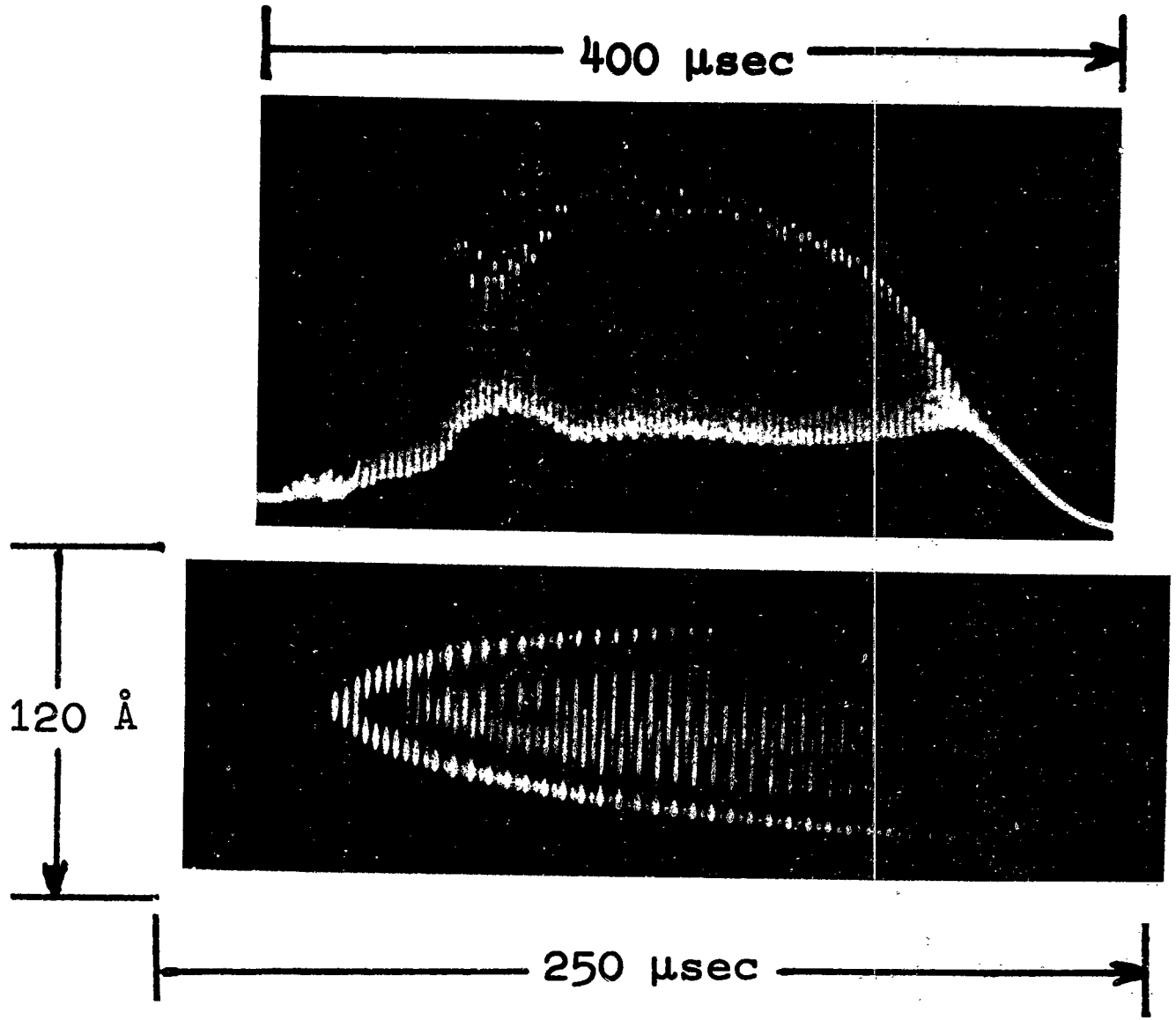

FIGURE 21. Time resolved spectrum and time trace for a 0.5 wt.% Nd_2O_3 laser glass at 77°K.

exit end of the laser is determined by coherent reflections from the end surface of the rod and the two surfaces of the plate. If the plate is misaligned or if the beam spread is sufficient the end of the rod has incoherently added to it a total reflectivity R due to the plate which is given by Eq. (3).

In Fig. 22 are shown the time resolved spectrum and time trace for the same rod as used in Fig. 19 but with a glass plate 2cm from the end of the rod. The plate was 0.5mm thick. The laser was pumped 100% above threshold at room temperature. The plate produces laser action at the wavelengths at which its thickness is an odd number of one-quarter wavelengths. The effect of the plate is superimposed on the hole burning. The irregularities in the time trace are correlated with the appearance of different portions of the spectrum. In Fig. 23 are shown the time resolved spectra for the same rod but with a 0.09mm thick mica plate 2cm from the rod. The lower frame was taken at 300°K and the upper one at 77°K. The two in the center are for intermediate temperatures. In the spectrum taken at 300°K the shift in emission toward longer wavelengths is due to heating of the mica plate. The room temperature emission occurs at the wavelengths of maximum reflectivity of the plate, but the spectrum at 77°K has an intensity distribution which follows the plate reflectivity. From the time resolved spectrum taken at intermediate temperatures it is evident that the broadening of the spectral emission occurs through hole burning steps. The width of the holes were less with the plate than without it.

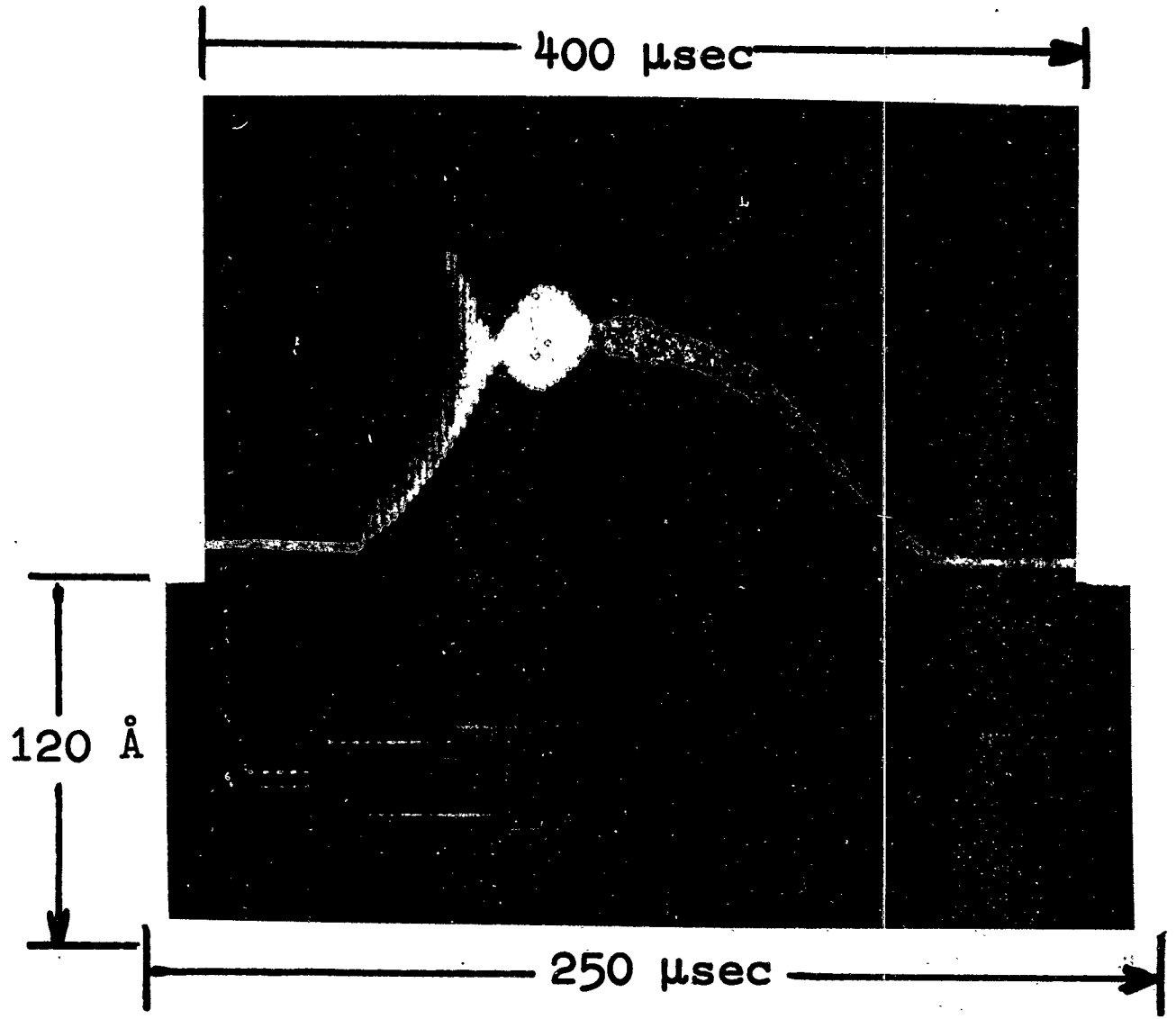

FIGURE 22. Time resolved spectrum and time trace for a 0.5mm thick glass plate 2cm from the end of the rod.

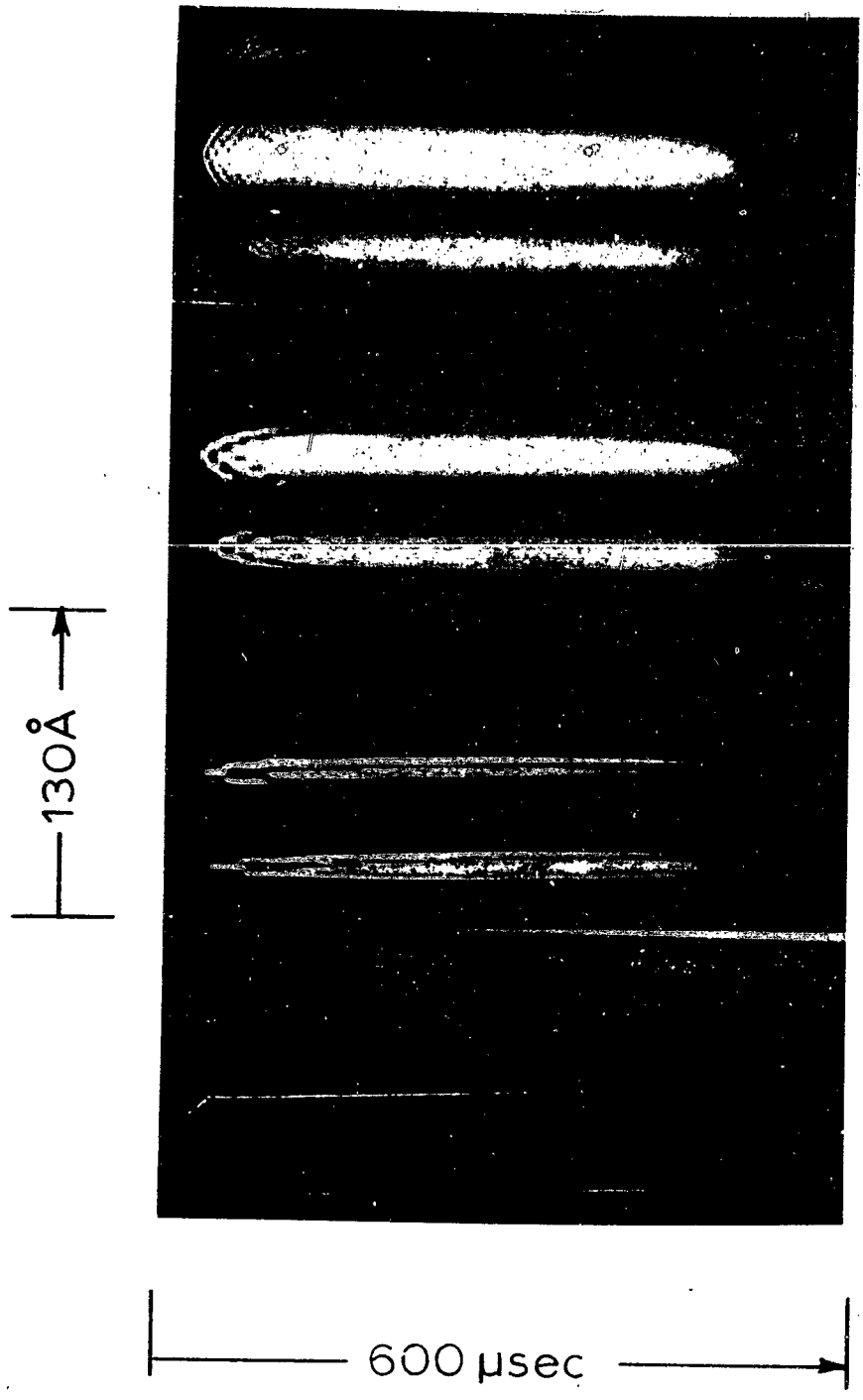

FIGURE 23. Time resolved spectra as a function of temperature with a 0.09mm thick mica plate 2cm from the rod. The lower frame was taken at 300°K, the upper at 77°K, and the center frames as the rod heated. The rod was pumped 100% above the room temperature threshold.

From the time resolved spectra, with and without reflecting plates, as functions of temperature and Nd^{3+} concentration the properties of the 180A wide line at 1.06μ can be described. Because of the large multiplicity of the final state there certainly must be a ligand field splitting such as shown in Fig. 24. For the sake of discussion, the terminal state is assumed to be split into three Kramers doublets. Each of these is inhomogeneously broadened due to slight differences in the field seen by different Nd^{3+} ions. There is not intended to be any correlation between corresponding positions in the three bands. For example, one ion could emit at ν', ν_a', and ν_c' and another ion also emit at ν' but with companion emissions at ν_a'' and ν_c''.

There is furthermore a homogeneous broadening of the line due to thermal effects. This would be of the same order as the width of the hole burned in the time resolved spectra. The smallest hole burned from Fig. 20 is 20A at 300°K and reduces to about 5A at 77°K. By taking a microdensitometer trace across the spectrum at 77°K for a rod that was pumped hard the shape of the inhomogeneous line can be obtained. This is shown in Fig. 25. The inhomogeneously widened line has a total width at one-half maximum of about 65A and extends slightly further to the long wavelength side.

In conclusion, the 180A wide line that occurs in spontaneous emission has an inhomogeneous broadening and ligand field splitting that are both 60-70A wide. The homogeneous thermal broadening is 20A at 300°K and narrows to about 5A at 77°K.

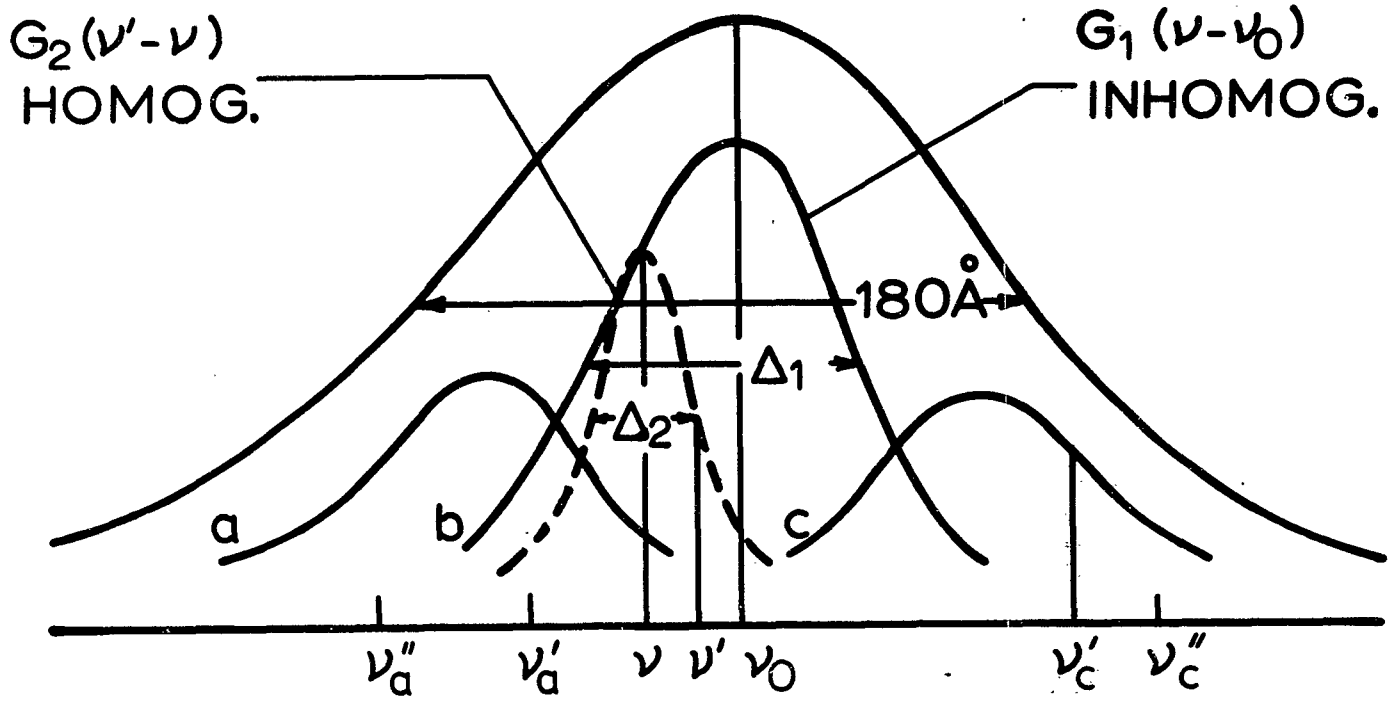

FIGURE 24. Schematic for the structure of the 180Å wide line emitting at 1.06μ. For the sake of discussion, the line is shown with a ligand field splitting into three Kramers doublets, an inhomogeneous broadening Δ_1, and a temperature dependent homogeneous broadening Δ_2.

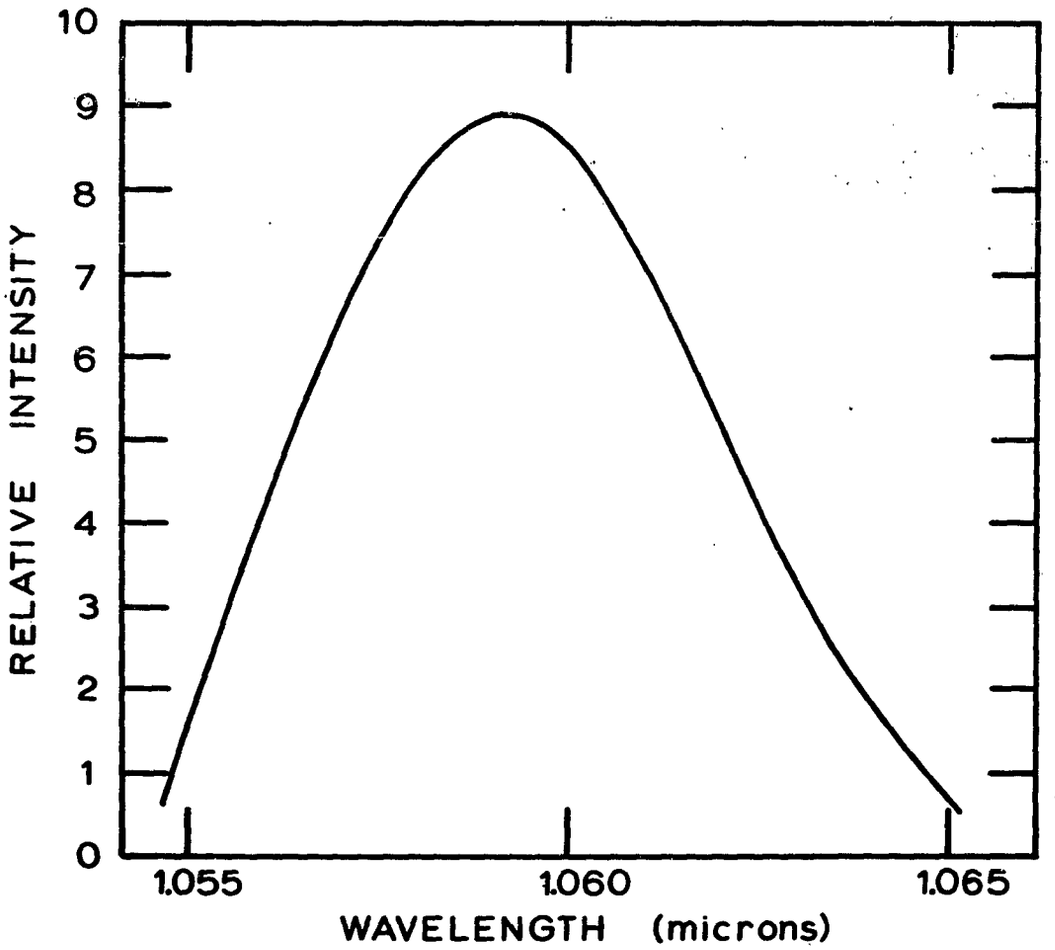

FIGURE 25. The relative intensity of induced emission as a function of wavelength at 77°K for a K-Rb-Ba-Si glass. The wavelength contour was taken 200μsec after emission began so as to avoid the region of initial transient oscillations. The pump power was eight times threshold.

IV. CALCULATION OF WAVELENGTH DEPENDENCE OF LASER EMISSION VS. TIME

To take account of the effects of homogeneous and inhomogeneous broadening it is necessary to handle equations like Eq. (9) and (10) for more than one frequency. The rate equations must be generalized to include a frequency dependence for the inversion and for the light in the cavity. The problem is similar to multimode oscillations considered by Statz and Tong[14], Hanken and Sauermann[18], and Pantell[19], but with the spatial cross relaxation replaced by spectral cross relaxation. Polarization and other effects discussed by Kikuchi[20] need not be taken into account, because the lack of coherence in the broad bands in effect averages these out.[21]

The rate equations as functions of the frequency ν for the inversion $N(\nu)$ and the laser light $J(\nu)$ for an unsaturated four-level system can be written as

$$\frac{dJ(\nu)}{dt} = -L(\nu)J(\nu) + \left[Af + BJ(\nu)\right] \int N(\nu')G_2(\nu'-\nu)d\nu' \qquad (29)$$

$$\frac{dN(\nu)}{dt} = p(t)G_1(\nu-\nu_0) - N(\nu)\left[Ah + B\int J(\nu')G_2(\nu'-\nu)d\nu'\right]$$
$$+ C\left[G_1(\nu-\nu_0)\int N(\nu)d\nu - N(\nu)\right] \qquad (30)$$

The cavity loss term can be written in terms of the Q by $L(\nu) = 2\pi\nu/Q(\nu)$. The pump term in Eq. (30) is assumed to follow the inhomogeneous distribution $G_1(\nu-\nu_0)$ centered on the frequency ν_0. The induced

emission terms in both equations are proportional to the Einstein B coefficients and depend on an integration over the homogeneous distribution $G_2(\nu'-\nu)$. The function G_1 is assumed normalized by

$$\int_0^\infty G_1(\nu-\nu_0)d\nu = 1 \tag{31}$$

and G_2 is taken as a Gaussian,

$$G_2(\nu'-\nu) = \left[(1n2)/\pi\Delta_2^2\right]^{\frac{1}{2}} \exp\left\{-(1n2)(\nu'-\nu)^2/\Delta_2^2\right\} \tag{32}$$

In Eq. (30) cross relaxation is assumed proportional to a single rate constant C and the deviation of the population distribution from the inhomogeneous distribution in an optically thin cavity with no laser light present. As in section IIIB the factor f takes account of the spontaneous emission into the solid angle about the rod axis that can be totally internally reflected, and it is given by $f = (n_1-n_2)n_2$, where n_1 and n_2 are the indices of refraction of core and cladding. The factor h gives the effect of non-radiative transitions and of radiation in other lines that start from the same upper state.

The frequency dependence of Eqs. (29) and (30) can be handled by breaking the frequency up into a finite number of intervals. Eqs. (9) and (10) are the result for a single frequency interval. If symmetry is assumed about the center frequency ν_0, the next most complicated case is for three evenly spaced light emissions centered on the inhomogeneous curve as shown in Fig. 26.

The unknowns are the three inversions N_1, N_2, N_3, and the three

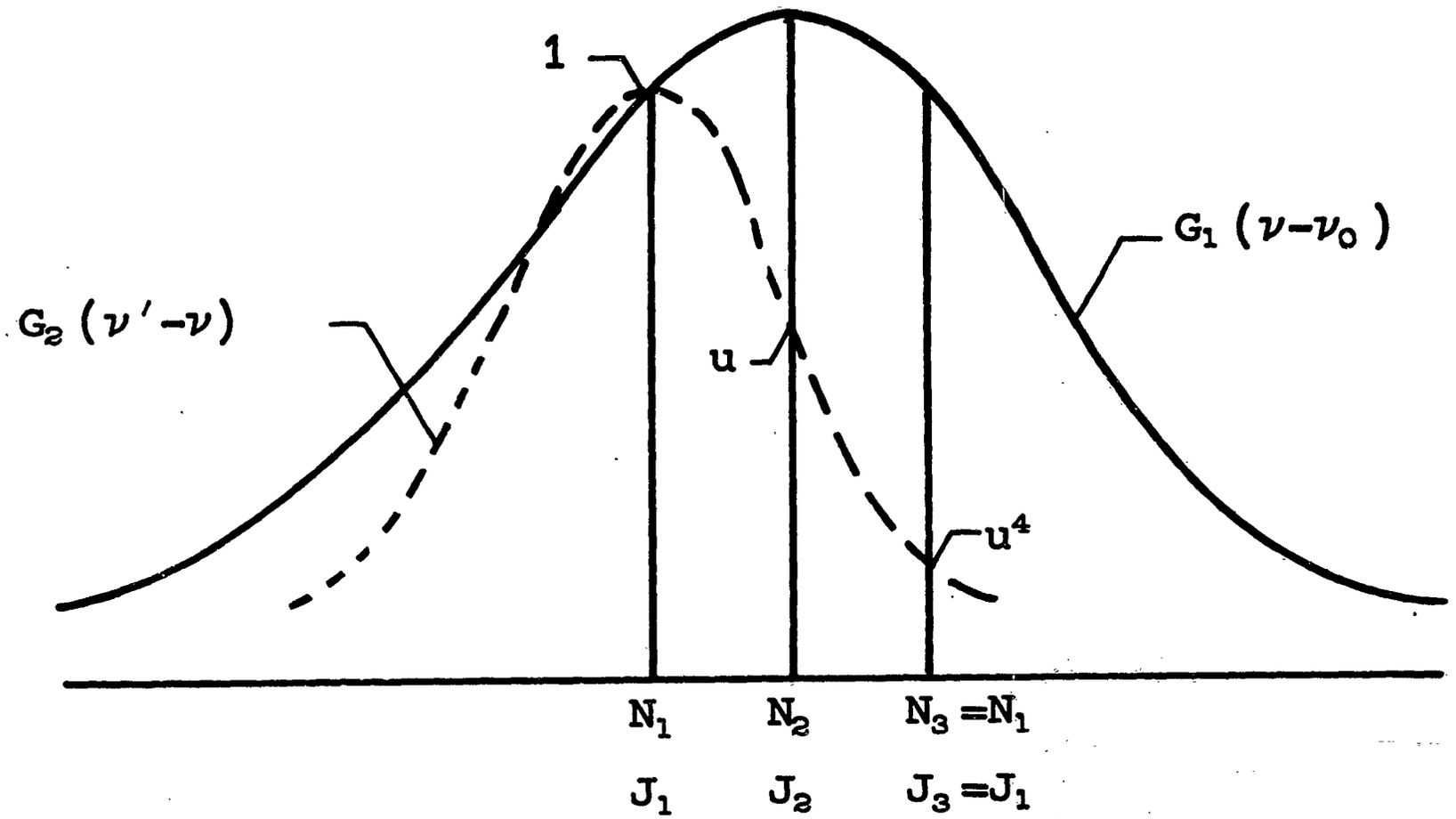

FIGURE 26. Schematic representation of the frequency dependence divided up into three evenly spaced wavelengths on the inhomogeneous curve $G_1(\nu-\nu_0)$. Symmetry is assumed so that $N_3 = N_1$ and $J_3 = J_1$. The homogeneous curve $G_2(\nu'-\nu)$ is a gaussian.

light intensities J_1, J_2, J_3. If the middle frequency is at the center of the line and if symmetrical initial conditions are assumed, then

$$N_3 = N_1 \text{ and } J_3 = J_1 . \tag{33}$$

The equations for the four unknowns are

$$\frac{dJ_1}{dt} = -LJ_1 + A(f + J_1 B/A)(N_1 + uN_2 + wN_3) \tag{34}$$

$$\frac{dJ_2}{dt} = -LJ_2 + A(f + J_2 B/A)(uN_1 + N_2 + uN_3) \tag{35}$$

$$\frac{dN_1}{dt} = P_1 - AN_1 \left[h + (B/A)(J_1 + uJ_2 + wJ_3) \right] + C \left[\frac{P_1}{2P_1 + P_2} (2N_1 + N_2) - N_1 \right] \tag{36}$$

$$\frac{dN_2}{dt} = P_2 - AN_2 \left[h + (B/A)(uJ_1 + J_2 + uJ_3) \right] + C \left[\frac{P_2}{2P_1 + P_2} (2N_1 + N_2) - N_2 \right] \tag{37}$$

In the above equations u gives the transition probability that light J_1 will cause induced emission of the ions N_2 and similarly w is the probability that J_1 induces emission at ν_1 of the N_3 ions. If the homogeneous line shape is assumed to be a Gaussian, the even spacing of the lines gives

$$w = u^4 \tag{38}$$

Laser emission will always occur at ν_2, but may or may not do so

at ν_1. The homogeneous line width, or its equivalent as represented by u, determine whether laser emission also goes in the wings at ν_1 and ν_2.

Consider the case where steady state has been reached so that $dI_1/dt = dI_2/dt = 0$. If emission occurs at ν_1 and ν_2, with sufficient pumping the spontaneous emission terms AfN_1 and AfN_2 can be neglected. The resulting equations with the left side zero and Af neglected give positive values for N_1 and N_2 only if

$$2u < 1 + u^4 \quad \text{or} \quad u < 0.567 \tag{39}$$

Hence it is reasonable to expect that the separation between two bands in the time resolved spectra would be about equal to the homogeneous linewidth.

Digital computer solutions of Eqs. (34) - (37) were obtained by relating the variables at time $t + \Delta t$ to their values at time t. For example, Eq. (34) would be written as

$$J_1\Big|_{t+\Delta t} = \left\{-LJ_1 + A(f + J_1 B/A)(N_1 + uN_2 + wN_3)\right\}\Big|_t \tag{40}$$

and similarly for Eqs. (35) - (37). To assure linearity a time interval Δt of 5×10^{-8} seconds was chosen, but with the computer set to print out only every twentieth point. The resulting data was then plotted to give the time variation of N_1, N_2, J_1, and J_2.

The number of parameters in Eqs. (34) - (37) can be reduced by converting the equations to dimensionless form, for example, by expressing time in units of t/L and relating the variables to their

threshold values. However, to preserve the physically intuitive scales for the variables, they are left as shown in the equations. The value of A is taken as $A = 0.5 \times 10^3 \text{ sec}^{-1}$. B/A is $(8\pi\nu^2/c^3n^3)^{-1}(2\Delta_2)^{-1}$ and was assigned the value $(2/3) \times 10^{-12}$. The cavity loss was assumed to be that for a 50cm long laser with a full reflector at one end and 4% reflectivity at the other; this corresponds to an average loss of 3.3%/cm, which gives a value of $L = 10^9 \text{ sec}^{-1}$. A good typical value for h is 3. These values for L, A, B/A and h were used throughout.

In Fig. 27 are shown the results from the computation with the additional parameters given the values C = 0, u = 0.1, $P_1/P_2 = 0.99$, f = 0.01, and P_2 is approximately twice threshold. Up to the times shown on the graph no laser light is present and the inversions N_1 and N_2 are increasing from zero at a linear rate. Laser emission first occurs at the center of the line J_2. The output is in the form of a damped train of relaxation oscillations. At each pulse of light N_2 decreases, but only slightly. This is because h is three and even during a laser pulse the inversion is only slightly lower. The value of n = 0.1 is small so that J_1 and J_2 are relatively uncoupled. The inversion N_1 continues to build up at a nearly linear rate until threshold is reached. Thereafter N_1 oscillates slightly similar to N_2. Emission in J_1 and J_2 at first tend to alternate as shown in Fig. 27. After approximately twenty pulses of light J_1 and J_1 are oscillating together and with continued time the oscillation slowly damps out. The distinguishing points of the case of weakly couple lines (u small) is that

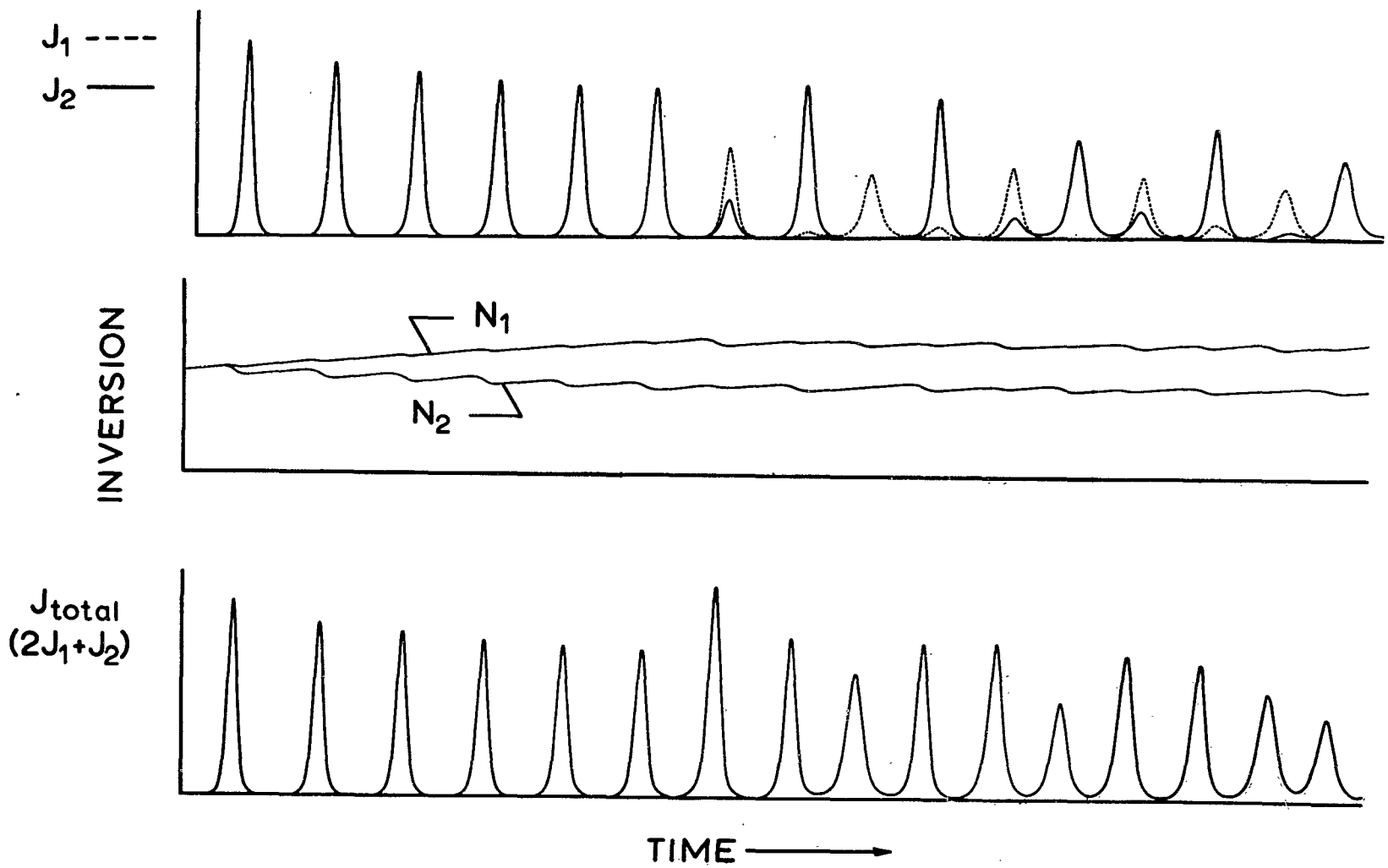

FIGURE 27. The results of a digital computer calculation of Eqs. (34) - (37) with the values of the parameters $A = 0.5 \times 10^{3}\,sec^{-1}$, $B/A = (2/3) \times 10^{-12}$, $L = 10^{9}\,sec^{-1}$, $h = 3$, $C = 0$, $u = 0.1$, $P_1/P_2 = 0.99$, $f = 0.01$, and P_2 is approximately twice threshold.

the light pulses in different spectral regions first alternate in intensity then pulse entrainment occurs in which the oscillations occur together, and finally the oscillations are damped out. In Fig. 28 is shown the same results for J_1 and J_2 as in Fig. 27 but with the frequency dependence made more evident.

In Fig. 29 is shown the results of a computation with the values of the parameters C = 0, u = 1/3, f = 0.1, P_1/P_2 = 0.9, and P_2 is approximately twice threshold. The strong damping results from the relatively large value of f.

There were sixteen runs made for various values of the parameters.

For reasonable values of C($< 10 cm^{-1}$) cross relaxation produced relatively little effect. Its major influence was to decrease the steady state value of N_1 when J_2 emission occurred.

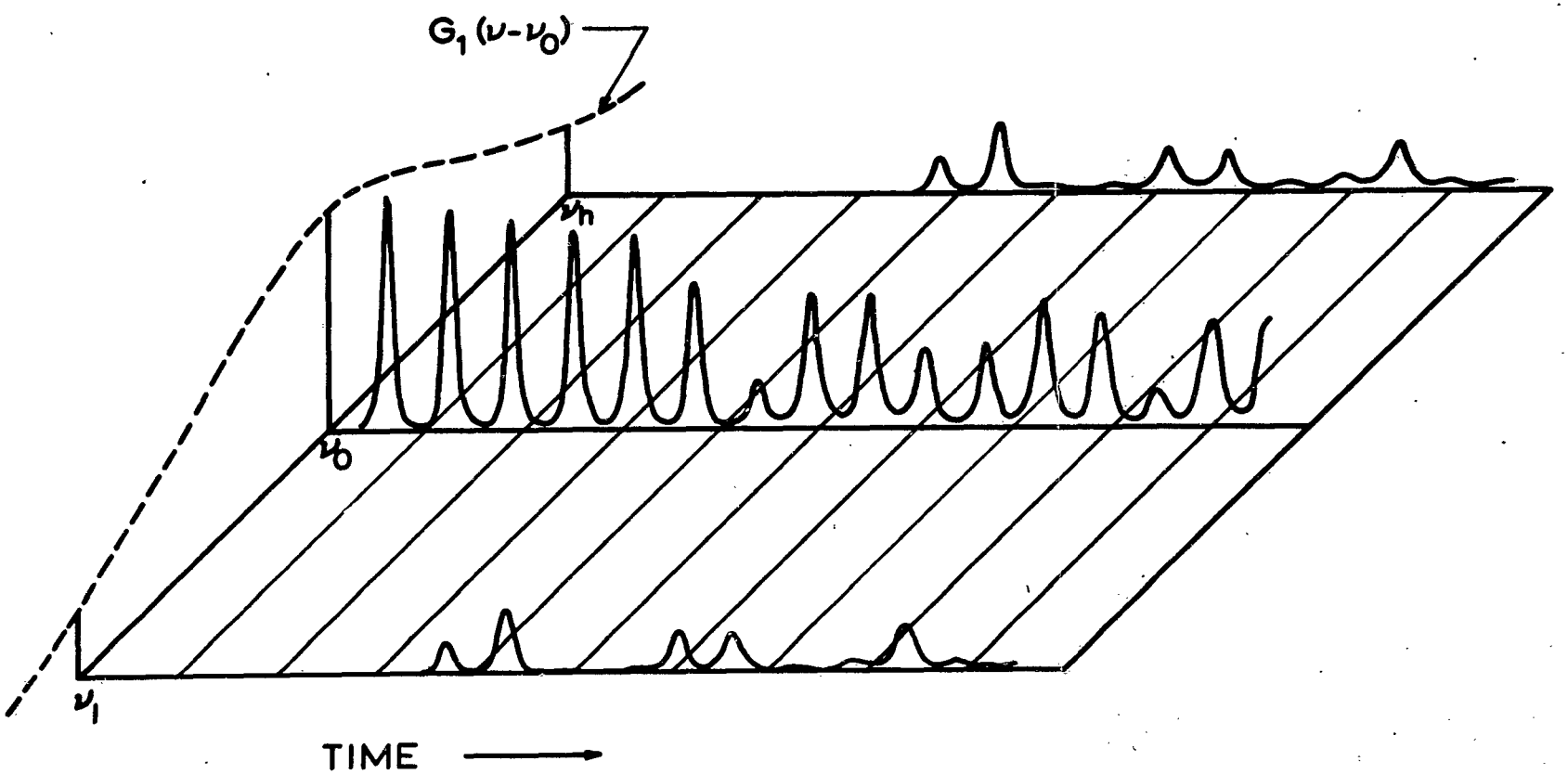

FIGURE 28. Computer solution for J_1 and J_2 with the values of the parameters A = $0.5 \times 10^3\,sec^{-1}$, B/A = $(2/3) \times 10^{-12}$, L = $10^9\,sec^{-1}$, h = 3, C = 0, u = 0.1, P_1/P_2 = 0.99, f = 0.01 and P_2 is approximately twice threshold.

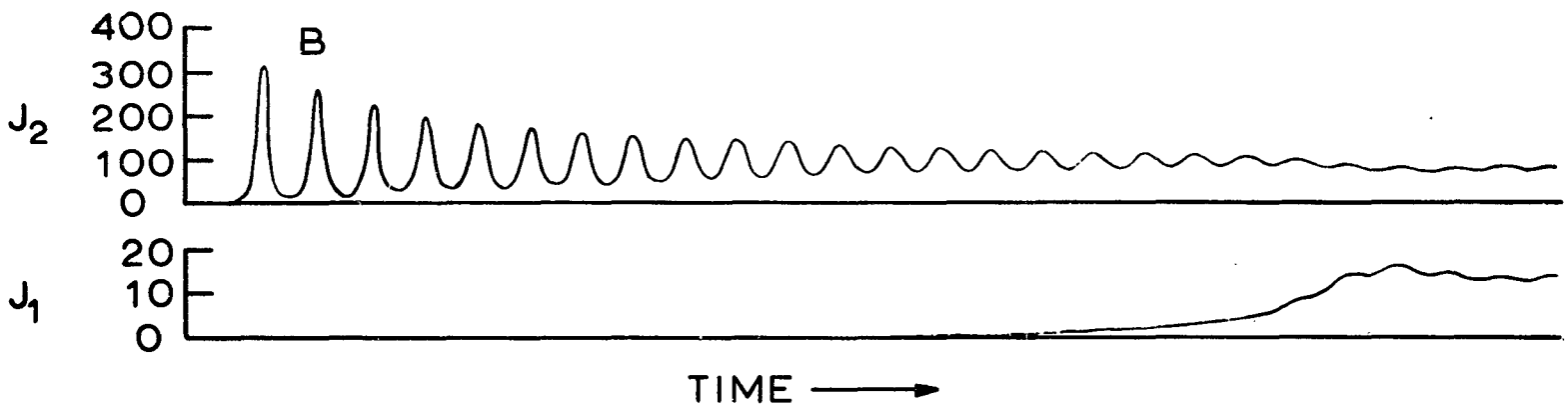

FIGURE 29. The results of computation for J_1 and J_2 from Eqs. (34) - (37) with the values of the parameters $A = 0.5 \times 10^3 \text{ sec}^{-1}$, $B/A = (2/3) \times 10^{-12}$, $L = 10^9 \text{ sec}^{-1}$, $h = 3$, $C = 0$, $u = 1/3$, $f = 0.1$, $P_1/P_2 = 0.9$ and P_2 is approximately twice threshold.

REFERENCES

1. E. Snitzer, 3rd Quantum Electronics Conf., ed. by P. Grivet and N. Bloembergen (Columbia University Press, New York, 1964), p. 999.

2. S.A. Collins and G.R. White, Appl. Opt. 2, 448 (1962).

3. M. Born and E. Wolf, Principles of Optics (Pergamon Press, London, 1959) p. 60.

4. A.W. Crook, J.O.S.A. 38, 954 (1948).

5. R.D. Mauer, Optical Masers, Microwave Research Institute Symposium Series 13, (Polytechnic Press, Brooklyn, New York, 1963) p. 435.

6. G.E. Peterson and P.M. Bridenbaugh, J. Optical Soc. Am. 54, 644 (1964).

7. R.W. Young, R.E. Graf, and N.M. Brandt, American Ceramic Society Meeting (Chicago, April, 1964).

8. P.B. Mauer, Appl. Optics 3, 153 (1964).

9. A.D. Pearson, S.P.S. Porto, and W.R. Northover, J. Appl. Phys. 35, 1704 (1964).

10. D.W. Harper, Phys. and Chem. of Glasses 5, 11 (1964).

11. R.F. Woodcock, J. Opt. Soc. Am. 53, 523 (1963).

12. C. Hirayama and D.W. Lewis, Phys. and Chem. of Glasses 5, 44 (1964).

13. H. Statz and G.A. de Mars, Quantum Electronics, ed. by C.H. Townes, Columbia University Press, New York, (1960), p. 530.

14. H. Statz and C.L. Tang, J. Appl. Phys. 35, 1377 (1964).

15. D.M. Sinnett, J. Appl. Phys. 33, 1578 (1962).

16. G. Makhov and O. Risgin, Proc. 3rd Quantum Electronics Conf., ed. by P. Grivet and N. Bloembergen (Columbia University Press, New York, 1964), p. 1121.

17. W.H. Keene and J.A. Weiss, J. Appl. Optics 3, 545 (1964).

18. H. Hanken and H. Sauermann, Z. Physik 173, 261 (1963).

19. R.H. Pantell, J. Appl. Phys. 35, 1404 (1964).

20. T.T. Kikuchi, J. Opt. Soc. Am. 54, 983 (1964).

21. C.L. Tang, J. Appl. Phys. 34, 2935 (1963).

Distribution List

Commanding Officer U. S. Army Research Office-Durham Durham, North Carolina	75
Commanding Officer Boston Procurement District, U. S. Army Attn: AMX BO-LD Army Base Boston 10, Massachusetts	1